1966

Influence of environment on the high temperature mechanical behavior of nickel alloys subjected to repeated stress

John Herbert Weber Jr.
Lehigh University

INFLUENCE OF ENVIRONMENT ON THE HIGH TEMPERATURE MECHANICAL BEHAVIOR OF NICKEL ALLOYS SUBJECTED TO REPEATED STRESS

by

John Herbert Weber, Jr.

A Thesis

Presented to the Graduate Faculty

of Lehigh University

in Candidacy for the Degree of

Master of Science

Lehigh University

1966

Certificate of Approval

This thesis is accepted and approved in partial fulfillment of the requirements for the degree of Master of Science.

16 Sept. 1966
(date)

F. Leibsch
Professor in Charge

F. Leibsch
Head of the Department

Acknowledgements

The professional guidance and inspiration provided by Professor Joseph F. Libsch, Head of the Department of Metallurgy and Materials Science, Lehigh University are gratefully acknowledged. The author is grateful for the assistance of Mr. Martin Sheska and the department shop staff in solving many technical problems.

The Weidemann Division of Warner and Swasey Company, Barber-Coleman Company, and Lepel High Frequency Laboratories have contributed to this project through technial assistance and loan of equipment. The author is indebted to the International Nickel Company for the production and fabrication of alloys used.

Mr. P. P. Podgurski and Mr. L. Salvage of Homer Research Laboratories, Bethlehem Steel Corporation are acknowledged for their technical assistance.

Finally, the author is grateful to the Materials Research Center, Lehigh University and the International Nickel Company, Incorporated for their financial support of this work.

Table of Contents

	Page
Certificate of Approval	ii
Acknowledgements	iii
Table of Contents	iv
List of Tables	vi
List of Figures	vii
Abstract	1
Introduction	2
Experimental Procedures	5
Materials	5
Test Equipment	6
A. Tension	6
B. Fatigue	6
B.1.) Temperature control	8
B.2.) Testing sequence	9
Analytical Equipment	10
A. X-ray	10
B. Metallography and Electron Probe	10
Results and Discussion	12
Tensile Behavior	12
Fatigue Behavior	12
A. Air atmosphere	13
B. Argon atmosphere	13
C. Atmospheric effects	15
X-ray Analysis	16
Metallography and Electron Probe Analysis	18
A. Cracking Behavior	18
B. Oxidation and its effects	19
C. Effects of solute elements	24
Summary	26

Table of Contents (cont'd.)

	Page
Conclusions	27
Further Work	28
Appendix I. Stress Calculation	29
Bibliography	30
Vita	62

List of Tables

Table		Page
I	Chemical Composition of Alloys- Weight Percent	34
II	Tensile Test Data	35
III	X-ray Diffraction Data	36
IV	Substrate Cracking Behavior	37

List of Figures

Figure		Page
1	Fatigue specimen	39
2	Fatigue testing equipment	40
3	Atmosphere test chamber	41
4	Sectioning for metallography	42
5	Fatigue data for nickel alloys tested in air at 1500° F.	43
6	Fatigue data for nickel alloys tested in argon at 1500° F.	44
7	Stress vs. Cycles to failure for pure nickel, Ni-Al, Ni-Be alloys tested in argon at 1500° F.	45
8	Comparison of fatigue behavior of pure nickel tested in air and in argon at 1500° F.	46
9	Comparison of fatigue behavior of Ni-Al alloy tested in air and in argon at 1500° F.	47
10	Comparison of fatigue behavior of Ni-Si alloy tested in air and in argon at 1500° F.	48
11	Comparison of fatigue behavior of Ni-Be alloy tested in air and in argon at 1500° F.	49
12	Macrograph of Ni-Be alloy showing typical surface view of fracture as tested in air (3.9×10^4 cycles), 15X.	50
13	Macrograph of pure nickel tested in argon (1.23×10^5 cycles). (a) surface slip in the grains, 14X, (b) surface roughness after testing, 5.2X.	50
14	Macrograph of Ni-Si alloy tested in air (8.19×10^5 cycles) showing typical intergranular fracture surface, 8X.	51
15	Macrograph of pure nickel tested in air (7.5×10^3 cycles) showing fracture of oxide layer, 14X.	51

List of Figures (cont'd.)

Figure		Page
16	Macrograph of Ni-Be alloy tested in air (1.01×10^7 cycles) exhibiting flaking of oxide layer, 12X.	52
17	Blunting of crack tips by oxide. (a) pure nickel tested in air (1.02×10^7 cycles), 200X, (b) Ni-Be alloy tested in air (1.0×10^7 cycles), 250X.	52
18	Micrographs of Ni-Al alloy tested in air (1.0×10^7 cycles). (a) grain boundary behavior as seen in the light microscope, 250X, (b) aluminum x-ray image showing aluminum concentrations at grain boundaries, 250X, (c) aluminum x-ray line scan of line AB of (a). Note: aluminum concentration at peak is 14%, approximately five times that of the bulk material.	53
19	Oxidation as a result of stressing in air atmosphere. (a) Ni-Al alloy (1.0×10^7 cycles), 50X, (b) Ni-Si alloy (1.0×10^7 cycles), 50X.	54
20	Micrographs of Ni-Si alloy tested in air (1.0×10^7 cycles). (a) internally oxidized region, 250X, (b) electron image showing structure, 250X, (c) silicon x-ray image showing silicon concentration at grain boundaries, 250X.	55
21	Micrographs of Ni-Si alloy tested in argon (7.46×10^6 cycles). (a) view of surface and adjacent region, 250X, (b) electron image, 250X, (c) silicon x-ray image, 250X. Note lack of silicon concentration at grain boundaries.	56
22	Micrographs of Ni-Al alloy tested in air (1.0×10^7 cycles). (a) dispersion of particles below the surface, 500X, (b) view transverse to that of (a), 500X.	57
23	Micrographs of Ni-Al alloy tested in air (1.0×10^7 cycles). (a) surface and subsurface oxidation, 250X, (b) aluminum x-ray image showing enhanced aluminum content in the region of high particle density, 250X.	58

List of Figures (cont'd.)

Figure		Page
24	Micrograph of Ni-Be alloy tested in air (1.0×10^7 cycles) showing features of transverse section after testing, 55X.	59
25	Micrograph of Ni-Al alloy tested in air (7.2×10^4 cycles). Note grain boundary behavior. Etch: $HF-HNO_3$, 34X.	60
26	Oxidation of unstressed material. (a) Ni-Be alloy, 500X, (b) Ni-Si alloy, 500X, (c) Ni-Al alloy, 250X.	61

Abstract

The effect of various atmospheres upon the 1500°F mechanical behavior of pure nickel, nickel - 5 atomic percent aluminum, nickel - 5 atomic percent silicon, and nickel - 5 atomic percent beryllium was studied. It was found that in an inert atomosphere, the repeated stress behavior is relatively independent of solid solution alloying effects and depends primarily upon the host metal.

Oxidizing atmospheres, on the other hand, were found to affect the behavior through several mechanisms. Surface oxide inhibits slip and subsurface oxygen penetration in the form of dispersed oxide particles was found to strengthen the alloys. Grain boundary solute concentration and corresponding depletion in adjacent areas was observed. The effect of these factors upon mechanical behavior is discussed.

Evidence suggesting an interrelation between creep and fatigue at elevated temperature is also presented and discussed.

Introduction

With the advances of technology, metal parts subject to repeated stress have been placed under very severe service, elevated temperature being very common. Recent theoretical discussions of fatigue failure have been concerned primarily with ambient atmospheric conditions (1 - 5). When higher temperatures are encountered, environmental conditions are of utmost importance. Present knowledge of behavior under repeated stress must be extended if design criteria are to be developed for metal usage under these conditions.

Previous work by this investigator (6) found that to understand mechanical behavior at elevated temperatures, the combined influence of several factors must be considered. These factors include stress, temperature, environment, and metallurgical structure.

A major problem in considering the influence of repeated stress at elevated temperature is the relation between creep and fatigue. Meleka (7) proposed several methods of evaluating combined fatigue-creep data. Even more important than this is some form of structural theory to correlate these variables. One such theory, proposed by Kennedy (8), is based upon the summation of two opposing effects: a.) work-hardening produced by deformation and b.) thermal recovery which takes place at high temperature. Interpretation of results would be based upon the fact that large concentrations of vacancies are produced during repeated loading. These vacancies could either soften or harden the material depending upon their interaction with dislocation movement.

Temperature may have a significant influence on the mode of fracture. The occurrence of both intergranular and transgranular fracture has been observed. This fracture behavior cannot be attributed completely to temperature, but depends also upon the combined effects of stress and environment. These last two factors are inseparable if the environment is not inert.

Corrosion affects the fatigue behavior of materials most severly if it occurs concurrently with the actual fatigue (9). McKay and Worthington (10) state that corrosion is detrimental to the fatigue resistance of a material. An outstanding exception to the influence of corrosion is oxidation. This phenomenon, affecting almost all metals at elevated temperatures, can be very beneficial at lower stress levels where sufficient time allows its occurrence. Surface oxide and internal oxidation can strengthen alloys, though simultaneous embrittlement can be harmful. In simple binary alloys, solute elements can combine with oxygen to form dispersed oxides (11), thus giving the materials added strength at elevated temperatures. Behavior of many alloys has shown that solute elements will often preferentially oxidize causing solute depletion in adjacent regions. The presence of this concentration inhomogeneity may considerably affect the resultant behavior of the bulk material.

Through a rather recently developed procedure, high temperature fatigue testing can be done with some assurance of reproducibility. Harper, et al (12) have developed a facility of relatively good diversification with respect to repeated stressing at elevated temperature. Adaptation of this equipment can provide the environmental control necessary for fundamental research in this field.

The present study was concerned with three major areas:

(1) An adaptation of the above equipment for environmental control was made by fabricating a suitable atmosphere chamber.

(2) Fatigue-type date were obtained for a series of solid solution nickel alloys as tested in both inert and oxidizing atmospheres at 1500°F. It was anticipated that this data would show the effect of different environmental conditions upon the mechanical behavior of these alloys at elevated temperature.

(3) Metallography and electron probe micro-analysis were performed on the above specimens to form a more quantitative means

of evaluating the design of materials for high temperature applications. This analysis considered both surface and internal oxidation and their effect upon solute concentration and metallurgical structure.

Experimental Procedures

Materials

Alloys of the following nominal compositions were selected: pure nickel, nickel - 5 atomic percent aluminum, nickel - 5 atomic percent beryllium, and nickel - 5 atomic percent silicon. These alloys were selected for several reasons: a.) All three major alloying elements have a greater tendency for oxidation than nickel and form alloys which are single phase, solid solutions at the temperature studied; b.) the relative atomic diameter of the alloying elements with respect to nickel, that is, aluminum, silicon, and beryllium, fulfill the requirements of having larger, approximately the same, and smaller atomic radii than nickel respectively, and c.) each of the elements has a more rapid rate of diffusion through nickel than nickel self-diffusion.

The selected alloys were produced by vacuum-induction melting and vacuum casting into four-by-four inch square cast iron ingot molds. These ingots were then forged at 2100°F to sections 3/4 x 3 inches wide and finally hot rolled to strip approximately three inches wide by three-sixteenths inch thick. The compositions of the alloys used are given in Table I.

Specimen blanks were cut from the hot rolled plate. After grinding, these blanks were machined to the specifications shown in Figure 1. This type of maximum-stress fatigue specimen was used by Feilbach (13). In this specimen, a stress concentration is present due to the reduced section. Feilbach calculated the concentration and found it to be relatively small. Calculation of the maximum stress in the reduced section was made using the strength of materials solution found in Appendix I.

Specimens were annealed at 1650°F for four hours to relieve stresses from machining and to produce a relatively uniform grain size in the four materials. It should be noted that although this annealing temperature produced a large grain

size, (average grain diameter 0.170 mm.), this characteristic was desired for better high temperature fatigue resistance (14,15).

This annealing treatment, although performed in an "inert" gas atmosphere, produced a thin film of oxide on the specimens. This film was removed by careful hand polishing of both flat and edge surfaces with a series of successively finer emery papers. At all times, care was exercised to insure that fine scratches left by the finest paper (4/0 grit) were parallel to the longitudinal axis of the specimen. Care was also taken to prevent marring the surface before testing as the sensing device for temperature control was a radiation pyrometer sighted on this polished surface.

Although the possibility of preferred orientation seemed slight, a pole figure analysis was made using a Siemens Texture Diffractometer. This apparatus is of the modified - Schulz type in which the azimuthal and inclination angles can be varied in a synchronous manner. Pole figues were taken from reflections of {111} planes obtained using zirconium-filtered molybdenum K_α radiation. Results of this analysis gave no indication of any preferred orientation.

Test Equipment

A. Tension

The absence of strength data on these alloys, only one of which is commercially produced, required tension tests. These were performed on an Instron tension-compression testing machine at room temperature and at 1500°F, the temperature of fatigue testing.

B. Fatigue

The equipment used for elevated temperature fatigue-type testing in air atmospheres was developed at Lehigh University (12). As the present study encompassed atmospheres other than air, some provision had to be made for the containment of an atmosphere about the specimen while testing was in progress. Modifications were made for this purpose.

The modified equipment is shown in Figure 2. It consists of: A.) a cantilever beam, reversed loading fatigue-testing machine; b.) a 2.0 Kw Lepel high frequency generator and its associated induction coil; c.) temperature control apparatus including a Wheelco - Land radiation pyrometer, a Wheelco Series 8000 temperature recorder, and a model MMC three-function current proportioning control unit; and d.) a stainless steel chamber for enclosing the atmosphere.

The cyclic loading is supplied by a Wiedemann-Baldwin SF-2 fatigue testing machine. This machine is capable of producing a load of $\pm$ 25 pounds maximum at a frequency of 1800 cycles per minute.

The stainless steel atmosphere chamber incorporated several basic ideas from the original equipment. The relative positions of the radiation pyrometer, specimen, and induction coil, shown in Figure 3, are similar to those in the original equipment. The most serious problem encountered was that of transferral of the cyclic load through the base of the chamber from the fatigue testing machine to the specimen. This was accomplished by use of a nickel bellows designed specifically for this purpose. To facilitate observation while testing, the face plate of the chamber was made of one inch Plexiglas. Minor modifications of this chamber permit testing in vacuum.

Heating of the specimen is accomplished by using an induction coil supplied with power through insulated leads in the chamber wall by the high-frequency generator.

Temperature control is maintained by the three components mentioned previously: the radiation pyrometer, the temperature recorder, and the three-function current proportioning control. The temperature is sensed by the radiation pyrometer sighted between two turns of the induction coil. This signal is the input for the temperature recorder which is connected to the current proportioning control unit. This unit controls the temperature through a silicon-controlled rectifier connected in series with an electronic servo-mechanism

which adjusts the power input to the induction coil.

B.1.) Temperature control

The presence or absence of oxides on the test specimens has a large effect on the emmissivities as seen by the radiation pyrometer. It was therefore necessary to use methods other than radiation pyrometry to determine the proper control setting for each alloy-atmosphere combination. Feilbach (13) states that this could be achieved through temperature calibration specimens identical to the test specimens with the exception of the addition of an iron-constantan thermo-couple welded onto them. This thermocouple was located on the under side of the specimens directly in the center of the reduced section.

A modification of this procedure was made due to difficulty encountered in trying to weld the wires to the specimens. Instead of the specimen forming the bead between the thermocouple wires, beads were formed between the wires themselves. These beads were placed in small holes drilled in the calibration specimens. Doubt as to the validity of this technique was dispelled when calibration procedures run on specimens containing both types of thermocouples showed little temperature difference between the two types of couples.

Thermocouples made of thirty gage (0.010 inches in diameter) wire were attached to the calibration specimen and temperature control was established with the specimen installed in the testing machine. The power setting on the controller was varied until a potentiometer attached to the thermocouple indicated that the specimen was at the desired temperature. The settings on the current control were then adjusted to maintain the temperature to a precision of $\pm$ 10° F. This procedure was followed each time the material-atmosphere combination was changed. Calibration specimens were used frequently to verify that temperature control was being maintained from test to test.

Another problem inherent in the use of thermocouples is their limited life during periods of specimen vibration. Feilbach (13) and Harper (16) examined this problem and state

that temperature change occurring during the switching from static to dynamic conditions was negligible. Hence, all calibrations were determined under static conditions.

A final consideration in temperature control is oxide formation on the specimens. To insure uniform conditions and stable temperature control in the oxidizing atmospheres, each specimen was held at test temperature for three-quarters of an hour prior to the start of dynamic testing. Identical procedures were followed for calibration and test specimens alike.

Atmospheres which were inert and produced no surface oxide were considered differently. In these tests, the chamber was flushed with argon for 45 minutes prior to heating the specimen. During the last fifteen minutes of this period, a "getter" of copper at approximately 1600° F. was used to absorb much of the reamining oxidizing components of the atmosphere. This procedure having been completed, the specimen was heated to test temperature for a ten minute soaking period after which calibration or testing was begun.

B.2.) Testing sequence

Fatigue-type testing was conducted at 1500° F. in two atmospheres. The first of these environments, air, was oxidizing to both the nickel and the major alloying element. In contrast to this behavior, the second environment, argon, was oxidizing to neither nickel nor the alloying elements.

The choice of the 1500° F. testing temperature was an attempt to optimize many different variables. A high temperature was desired for rapid diffusion and higher oxidation rates. Also, the temperature was chosen high enough to keep the alloys in the solid solution condition. Offsetting these reasons for high temperature were the necessity to keep the temperature low enough to prevent excessive grain growth and to permit higher testing stresses for accuracy of load application.

Temperature control, mentioned previously, exhibited a maximum reliable precision of 1500° F. ± 10° F. Dunsby (17)

in his evaluation for furnace requirements for elevated temperature testing found that no standard criteria appear to exist for this type of fatigue testing. Interaction between creep and fatigue should be considered under the given testing conditions.

Analytical Equipment

A. X-ray

Since the nature of the specimen surface with respect to oxide formation had a significant influence on the mechanical behavior, an X-ray diffraction analysis was made using a.) polished, heat-treated material prior to testing, and b.) reduced sections of specimens tested for the longest lifetimes in air and argon. From the untested material, the lattice parameters of the alloys were determined. The presence and types of oxides were determined from the tested material.

Equipment used in this analysis was a Siemens Kristalloflex IV X-ray unit and corresponding instrumentation for counting and recording the reflected radiation. Radiation used was zirconium-filtered molybdenum K_{α}.

B. Metallography and Electron Probe

Representative samples for both metallographic and electron probe analysis were selected from each alloy-atmosphere combination. These specimens were examined microscopically in the as-tested condition in an effort to understand the gross features of the phenomena occurring. The reduced sections were then removed and cut into two pieces. One of these pieces was mounted to allow observation of the flat surface of the specimen, while the other was mounted to produce a transverse view of the thickness. The orientations of these sections with respect to the specimen are clearly shown in Figure 4. This procedure was followed for two reasons: first, in the fatigue-type testing of this study, the reduced section of the specimen is the portion most affected, and second, effects throughout the thickness must also be considered .

Polished section examination indicated that further evaluation with the electron probe might provide insight into the oxidation behavior. A Cambridge Model Mark IV Electron-probe Microanalyzer was used for this analysis. Three types of data were produced: electron images, elemental X-ray images, and X-ray line scans. Note should be made that on specimens of the nickel-aluminum alloy used for probe analysis, powdered magnesium oxide instead of alumina was used as a grinding powder on the laps. This change was necessitated by the erroneous results which would have been produced on aluminum X-ray images by the aluminum-alumina combination.

The final step was to etch the polished specimens and examine the resulting microstructures. The etchant used was composed of twenty milliliters concentrated nitric acid mixed with fifteen drops hydrofluoric acid. This etchant was found to provide suitable structural observations using etching times between one and ten seconds.

Fatigue specimens were not the only type examined in the above manner. Due to the presence of oxide on many of the fatigue specimens, a similar microstructural analysis was performed on oxidized but unstressed samples. These specimens were produced by heating coupons of each alloy at 1500° F. in a static air atmosphere for approximately 100 hours, this period of time being equivalent to an endurance life of about ten million cycles. The characteristics exhibited in these samples were aids in the evaluation of the inter-related effects of high temperature behavior and oxidation.

Results and Discussion

Tensile Behavior

Tensile tests were performed on all four alloys at both room temperature and 1500° F., the fatigue testing temperature. Data for pure nickel were found in the literature (18) and used as a comparison for the test results obtained. The present data and that found in the literature are found in Table II. The data reported for 1500° F. were obtained from single specimens of each material tested in air and, although the relative magnitudes of the strengths are probably correct, values should be considered preliminary. The data at room temperature were obtained from duplicate specimens and reported as averages of two values .

Several factors should be noted about this tensile data. The addition of alloying elements increased the strength of the pure nickel significantly. At room temperature the alloys are, in order of increasing strengths: pure nickel, nickel - aluminum, nickel - silicon, and nickel - beryllium. This order changed at 1500° F., in that the tensile strengths of the nickel - aluminum and nickel - silicon alloys showed a reversed order.

The ductility of these materials, as evaluated by percent elongation, was found to decrease when tested at the elevated temperature. In all cases, elongation at room temperature was approximately fifty percent, while at 1500° F. only the nickel - beryllium alloy indicated a possibility of obtaining an elongation in excess of twenty-five percent. This decrease in ductility has been previously noted by Lozinskiy and Pertsovskiy (19).

Fatigue Behavior

Fatigue-type data were obtained for pure nickel, nickel - 5 atomic percent aluminum, nickel - 5 atomic percent silicon, and nickel - 5 atomic percent beryllium at 1500° F. in

atmospheres of air and argon. Figure 5 shows a plot of stress verses logarithm of cycles for all four alloys as tested in air. Similarly, Figure 6 shows the data for the alloys as tested in argon.

A. Air atmosphere

Figure 5 presents two phenomena to be considered. For an endurance life of approximately ten million cycles, the four materials show strengths which have the same relative order as the 1500 ° F. tensile strengths; that is, in order of increasing strengths: pure nickel, nickel - silicon, nickel - aluminum, and nickel - beryllium. At shorter lives this order is maintained with only one exception. Clearly, the nickel - beryllium alloy exhibits a behavior which makes it a poor choice for short time life. A plausible explanation of this behavior is discussed in a later section in view of metallographic observations made.

B. Argon atmosphere

Mechanical behavior in argon showed a striking difference. Figure 6 shows that, with the exception of the nickel - silicon alloy, the mechanical behavior of all alloys is identical and that there is no correlation with the static tensile properties. This behavior was surprising as one would expect that, under these inert conditions, the effect of the solid solution hardening should be noted.

Present theories of creep can, however, explain the similar behavior of these materials in the argon atmosphere. The effect of solute elements upon the creep behavior of the solvent material can be related to the competition between their effect upon the rates of work-hardening and recovery (21). At temperatures, $T \leq 0.50\ T_{mp}$ (the melting point of the material), where the rate of strain hardening is increased significantly, alloying is seen to have a beneficial effect upon creep resistance; but at temperatures where recovery is more rapid, solid solution strengthening has little effect (22). Since the temperature of testing in this study is of the order of $0.63\ T_{mp}$ of nickel,

the importance of creep on mechanical behavior is indicated.

Observation showed that specimens of the nickel - silicon alloy tested in argon for a life of greater than 500,000 cycles had a visible layer of oxide in spite of the "inert" atmosphere. Although this layer was superficial, later discussion will demonstrate that surface oxidation improved mechanical behavior at longer endurance life.

The similarity in behavior of the alloys in the argon atmosphere led to an attempt to derive an empirical equation for this situation. In the low-cycle range, fatigue-type data have often been plotted with coordinates of logarithm of total strain verses logarithm of life (in cycles). This idea proposed by Basquin (20) was used in conjunction with a least squares analysis. Basquin proposed that this law, given by

$$\ln S = \ln k - m \ln N$$

where

S = stress

ln k = constant

N = life, in cycles

would hold true for fatigue testing in general. In the present case, the relationships obtained were the following:

a.) for the pure nickel alloy

$$\ln S = 12.072 - 0.251 \ln N$$

b.) for the nickel - aluminum alloy

$$\ln S = 12.256 - 0.267 \ln N$$

c.) for the nickel - beryllium alloy

$$\ln S = 11.985 - 0.250 \ln N$$

Plotting and analyzing the data from these three alloys collectively would result in the plot shown in Figure 7. Although the straight line

$$\ln S = 12.040 - 0.251 \ln N$$

can be derived for this collective data, the important consideration here is that all of the data fits within a band of relatively narrow width. This is especially significant when considering that fatigue-type data inherently show a reasonable amount of scatter.

C. Atmospheric effects

Very important in this study of elevated temperature mechanical behavior are the results obtained from the curves shown in Figures 8 to 11. First, note that in all cases except the nickel - aluminum alloy there exists a crossover of the curves for the two atmospheres. The presence of this phenomenon leads to the conclusion that for higher stress levels the general trend is for the materials to have greater endurance in argon, while the reverse is true at lower stress levels. Similar behavior has been noted before (23 - 25) although reservations were encountered as specimen thickness seemed to be an important factor. Since the specimen thickness used in this study is several times the "critical thickness", this factor should be relatively unimportant.

The number of cycles at which crossover takes place seems to follow qualitatively the relative ease with which the solute element in the alloy is oxidized. Considering free energy values (26) as a rough measure of oxidation tendency, it was found that the order of the major alloying elements with respect to decreasing oxidation tendency was aluminum, silicon, beryllium, and nickel. The resulting rationale is that with the addition of an alloying element which oxidizes more readily than the host metal, nickel, the range of endurance life for which the inert atmosphere is superior to an oxidizing atmosphere decreases. The amount of this decrease is qualitatively proportional to the ease with which the alloying element may be oxidized. It should be realized that this can be, at best, only a "rule of thumb" as the activities of the alloying elements in the solid solutions, which are at present unmeasured for these alloys, were not considered.

The crossover indicates the existence of several mechanisms occurring during the testing in the different atmospheres. In particular, this can easily occur during testing in oxidizing atmospheres and has been previously suggested (23, 24, 28, 29).

These mechanisms are: (a) Adsorption of gas atoms on the specimen and especially on crack surfaces, tending to lower the surface energy of the material and permitting easier propagation of the crack; and (b) the reaction which forms oxide, which usually decreases and in some cases stops propagation, thus increasing the endurance life.

The data presented support this hypothesis. For short endurance life, the adsorption of gas atoms is the dominant mechanism as oxide in sufficient amounts has not had sufficient time to form. The strengthening abilities of the oxides formed are manifested only during longer endurance life, when the oxide, due to its superior strength at elevated temperatures, strengthens the material. Of course the metal-oxide bonding is a critical factor during this period. Cass and Achter (25) examined this bonding and found it to exhibit sufficient strength for the above mechanism to be possible.

The nickel - aluminum alloy shows a slightly different behavior in that no crossover is found. The proposed hypotheses can also account for this pattern. For example, the relatively high free energy of the reaction of aluminum combining with oxygen to form alumina suggests that the range over which specimens tested in argon may exhibit better behavior may be drastically reduced. Due to the possibility of very rapid aluminum oxidation, the oxide necessary for strengthening can be formed very quickly. Hence, the "gas adsorption mechanism" is completely overshadowed.

X-ray Analysis

One portion of the X-ray analysis consisted of scanning specimens with a diffractometer. The purpose of these scannings was to evaluate the structure and lattice parameters of the alloys and their oxides. Three scannings were made on each of the four alloys from specimens having conditions of a.) base material, heat-treated but prior to testing, b.) tested for approximately 10^7 cycles in the air atmosphere, and c.) tested for approximately

10^7 cycles in the argon atmosphere. Pertinent results of this study are found in Table III.

First consider the data obtained from the base materials. For the pure nickel, the structure was face-centered cubic with a lattice parameter a_o of 3.529 Å. Similar analyses on the three alloys produced data which also indicated face-centered cubic materials and gave the conclusion that the alloying element is found as substitutional atoms in the lattice of the solvent nickel. Logically, it would be expected that the addition of larger or smaller solute atoms would increase or decrease, respectively, the lattice parameter of the solvent material. This was found to hold true.

Most important to the present study was the second set of specimens; those tested in <u>air</u> for the longest life. The oxide and type of oxide formed on these specimens were particularly pertinent in evaluating the previously mentioned mechanical behavior. In these cases, the oxide was found to be a face-centered cubic structure of the NaCl type. This structure had previously been found for pure nickel oxide (30, 39). The fact that the three binary alloys showed a similar structure indicates that again the alloying elements are in substitutional positions with respect to the nickel atoms. The relative atomic sizes of the alloying elements with respect to nickel affected the oxide lattice parameter in a similar manner to that found in the alloys themselves.

X-ray diffractometer analyses obtained from the specimens tested in <u>argon</u> showed different behavioral trends from those noted for specimens tested in air. Pure nickel and the nickel - aluminum analyses showed only peaks resulting from the base materials. This indicates that any surface layers or oxides formed during testing were too thin to diffract x-ray radiation in sufficient quantities to produce visible peaks above the background radiation level. It does not preclude the existence of these layers, as will be discussed later. The oxide seen on the nickel - silicon alloy during the long-life testing in

argon was evident in the X-ray analysis of this specimen, although even in this case the intensities of the oxide peaks were very small compared with those of the alloy itself.

The nickel - beryllium alloy showed a significant departure from the behavior of the other materials. X-ray diffraction analysis of the argon-tested specimen showed at least two sets of correlated peaks, the strongest being of the base material. The positions where the oxide peaks might have occurred showed some slight indication that the necessary oxide thickness for visible peaks above background may have been attained. Most unusual was a set of peaks which indexed to be a face-centered cubic material of lattice parameter 3.527Å. The presence of these peaks discloses the existence of a material having the same structure and a similar lattice parameter to that of the pure nickel. Efforts to obtain an explanation for the presence of this phenomenon using metallography and electron probe analysis were unsuccessful.

Metallography and Electron Probe Analysis

A. Cracking Behavior

The first observation made of every specimen was of the as-tested surface. In the cases of the argon-tested and short-time air-tested specimens, direct observations of the cracks and specimen surface could be made. Observations on long-life air-tested specimens were more difficult and required removal of the oxide layer before cracking of the base material could be observed.

Several general trends were found with respect to the number of cracks and the presence or absence of branching of these cracks (see Table IV). Previous investigators (31, 32) have found that the number and type of cracks formed during high temperature repeated stressing are dependent upon many factors, several of which are: stress amplitude, mean stress, cycling frequency, temperature, environment, and metallurgical structure. The three factors pertinent to the present study are: stress amplitude, environment, and metallurgical structural changes

effected by the environment.

Both environments, at high and low stress levels, produced many cracks in the pure nickel material. The higher stress levels exhibited crack branching, while the lower levels showed little or no branching at all. The similar cracking characteristics of pure nickel specimens tested in the two atmospheres may be partially attributed to the problem of grain growth. At the testing temperature used for example, evidence showed that secondary recrystallization occurred in the pure nickel.

The influence of atmosphere upon the cracking behavior of the binary alloys was most evident with long endurance life. While specimens tested for short endurance life in both atmospheres showed branching of only a few major cracks (see Figure 12), those tested in air for long times showed many cracks as previously predicted (9) and reported by Danek, et al (23).

In addition to the observations recorded in Table IV, the pure nickel exhibited another striking behavior in the argon atmosphere, that is, deformation in the grains. The evenly distributed surface slip in many of the grains, Figure 13a, is a known feature of deformation at elevated temperatures (34, 35). The resultant effect of this deformation in the grains and the relatively large grain size of the material produced the extreme roughness of this specimen (see Figure 13b).

The metallic failure mode was completely intergranular in nature. The term "equicohesive temperature" has been used in the early literature relating to elevated temperature behavior. This term was used to designate that temperature, under the given testing conditions, where the cohesive strengths of the bulk granular material and the grain boundary material were equal. Obviously in the cases studied, this temperature has been exceeded. Figure 14 shows a typical transverse view of an intergranular fracture surface.

B. Oxidation and its effects

The evaluation of these different cracking phenomena is

dependent upon many interrelated factors. A consideration of the effect of oxide formation on the specimen surface is imperative. Figure 15 shows a typical surface view of a specimen of pure nickel tested in air at a high stress level. This picture shows the fracturing of the oxide normal to the maximum bending stress.

The presence of oxide on the surface or in grain boundaries can strengthen the base material at elevated temperatures. Three methods of oxidation strengthening are known: (a) before cracks develop, a surface oxide layer may act as a barrier to surface slip; (b) oxidation can reduce the rate or stop crack propagation by blunting the crack tips; and (c) internal oxidation can strengthen the material (28). All three of these mechanisms were encountered in this study.

The first mechanism, that is, formation of a surface oxide which inhibits plastic deformation, is shown in a comparison of Figures 13 and 15. McHenry and Probst (33) made similar observations. The inhibiting behavior of the oxide is dependent upon its adherence to the base material and also upon the nature of the oxide itself (36). Several conditions, one of which is the relative specific volumes of the oxide and the base metal, have a strong effect on the adherence of the oxide (37). Calculations of the above showed that in all cases the oxide had a greater specific volume than the base metal. This provides some support for the existence of adherent oxides on the specimens tested. Nickel alloys, in general, show this tendency toward adherent oxides at temperatures greater than 1200°F. (10, 38, 40).

Actually, good adherence of the oxides was found in all the alloys tested except in the case shown in Figure 16 where the oxide has undergone some flaking. This may have been due to rapid cooling from testing temperatures, although it was only found in specimens of the nickel -beryllium alloy tested at the lowest stress levels. Another feature of Figure 16 is the presence of a second oxide layer (lighter areas) beneath the

flaked-off oxide. The existence of two-layered oxides on nickel alloys has been reported (38, 41) but, in the present study, little evidence other than that illustrated above was found.

A second type of strengthening is produced by crack blunting. Figure 17a shows a view of two cracks observed in a pure nickel specimen tested in air for a long endurance life. Note that the tip of the longer crack has been blunted and that the crack itself has been filled with oxide. The binary alloys, for example nickel - beryllium Figure 17b, also exhibited this pehnomenon. This behavior nicely illustrates the oxide strengthening mechanism which slows crack growth. Of course, if the oxide slows or stops crack growth, more cracks will be initiated and start to grow. In this manner, the many cracks seen in the long endurance life air-tested specimens can be formed.

The crack blunting mechanism is also dependent upon the mechanical properties of the oxide in the cracks. For the blunting process to occur without fracture of the oxide, the oxide must be much stronger than the metal itself or it must show sufficient ductility to withstand the cyclic straining without rupture.

The electron probe microanalyzer was very useful for observations relating to oxidation. Grain boundary segregation prior to testing can affect oxidation and fracture significantly (42). The greater tendencies of the alloying elements to oxidize suggest that existence of grain boundary oxide would be accompanied by increased solute content in the boundaries. The nickel - aluminum alloy as-tested in air, Figure 18, supports this suggestion. The concentration of aluminum in the alloy is seen in the aluminum X-ray image, Figure 18b, where the aluminum concentration is proportional to the density of white spots. An aluminum x-ray line scan, Figure 18c, of the line AB crossing a grain boundary seen in Figure 18a clearly shows the differences of concentration between the grain boundary material and the bulk material. This type of solute concentration, found in the binary alloys, indicates the presence of grain

boundary oxidation. In contrast, a probe analysis of the heat-treated, but untested materials showed no indication of solute segregation at the grain boundaries.

The third strengthening mechanism, that is, internal oxidation is influenced primarily by the same factors as grain boundary oxidation. The most important of these conditions, that is: (a) the nature and concentration of ions in the grain boundaries; (b) existence of nucleation sites; and (c) presence of sufficient oxygen, suggest that oxygen must diffuse relatively rapidly (46). The controlling process for surface oxide formation is also important to internal oxidation. In nickel alloys, this process can be either diffusion of nickel through the oxide (25, 44, 45) or diffusion of oxygen ions (10, 46, 47) into the base material.

Depletion of solute concentration precedes both bulk and grain boundary oxidation. Hence, the diffusion rates of the solute elements combined with their rates of oxidation must greatly exceed that of the nickel atoms. At 1500° F., the solute elements used in this study do have higher diffusivities than nickel (27, 48, 49).

Deep penetrations of oxygen along interior grain boundaries were found in many of the air-tested specimens of the binary alloys. Examples of this are shown in Figures 19a and 19b, specimens of the nickel - aluminum and nickel - silicon alloys, respectively. A close-up view of the central portion of Figure 19b is seen in Figure 20a. Abnormalities in the grain boundaries are clearly evident in the electron image, Figure 20b. A most important feature is the concentration of the alloying element, silicon, shown in the x-ray image, Figure 20c. Quantitatively the grain boundary concentration of silicon was approximately four times the concentration in the bulk material. This increase in the intergranular regions indicates the presence of an oxide of much higher silicon content than that found in the surface layer. This concentration also results in corresponding solute depletion of adjacent areas. These

depleted regions exhibited concentrations approximately one-half that in the bulk material.

The results thus far have presented evidence verifying the presence of variations in solute concentrations, but no proof has yet been given to evaluate whether this effect is caused by oxidation alone, stress alone, or a combination of both. A microprobe analysis was made on a specimen of the nickel - silicon alloy tested in argon. Figure 21a shows a photomicrograph of the selected area. Structural abnormalities are seen in the electron image, Figure 21b. An examination of the silicon x-ray image, Figure 21c, shows the grain boundary concentration of silicon to be negligible compared to that in the heavily oxidized specimen (see Figure 20c). Recalling that these long time argon tests showed a slight amount of surface oxide explains the probable cause for the small concentrations which can be found. This evidence indicates that the solute element concentrations have been caused primarily by oxidation alone.

The exact nature of the oxygen penetration just below the surface oxide was examined closely. A specimen of the nickel-aluminum alloy, Figure 22a, shows finely dispersed particles in crystallographic orientations. A perpendicular view, Figure 22b, also shows this behavior. Wolf, et al (11) reported that similar alloys have a subscale morphology of oriented acicular particles of oxide. These particles were formed by selective oxidation of one constituent in the alloy. As already discussed, solute concentrations are a result of oxidation. Hence, if the particles observed are oxide, regions containing a high density of these particles should show increased solute concentration. This is clearly demonstrated by Figure 23.

Transverse sections of many specimens showed a striking grain boundary behavior other than internal oxidation (see Figure 24). Voids located in the grain boundaries of these specimens enabled the granular structure of the alloys to be

seen in the unetched sections. The absence of this grain boundary delineation at the center of the specimens gave some indication of why these markings appear. Recall that the specimens have been tested in reversed bending and that the central portion of the specimen, that is, near the neutral axis, has not been subjected to the flexural loading. Hence, stress may play some part in causing this phenomenon. Mullendove and Grant (42) state that during fatigue at high temperatures and low stresses, voids can be formed at grain boundaries without failure. Another investigator correlates these voids with instantaneous creep (43).

Similar behavior to that above was also seen in nickel - aluminum specimens, Figure 25, tested for short endurance life in air. This delineation was also exhibited by binary alloy specimens tested in argon. Thus, the grain boundary markings appear to be a separation resulting from structural changes caused by the testing stresses and are found to occur independently of oxidation (35).

C. Effects of Solute Elements

The oxidation behavior of the binary alloys under static unstressed conditions helped to serve as a key to the effects of alloying elements. Figure 26 shows transverse views of the oxidation layers formed on the alloys. Note that the subscale penetration into the nickel - silicon alloy, Figure 26b, is much smaller than that shown by the other two alloys. This appears to be a result of increased resistance of the surface scale to penetration by the oxygen ions caused by the silicon alloying addition (11). The nickel - aluminum alloy, Figure 26c, has a thinner surface scale and exhibits a deeper subscale penetration. These behaviors are the combined effect of the relative atom size and the greater tendency toward oxidation of the solute elements as compared to those of the host metal.

The most pronounced effects of the solute elements are manifested in the comparative behavior of the binary alloys in the air and argon atmospheres. Their influence is

negligible when the alloys are used in the inert argon environment at elevated temperatures (see Figure 6). The significant value of alloying is realized when the materials undergo long periods of stressing in oxidizing environments. The relative tendency toward oxidation of the alloying element compared to that of the host metal qualitatively defines the endurance range over which the effect of the solute element is beneficial to the elevated temperature behavior under repeated stressing (see Figures 8 to 11). For example, the point corresponding to the endurance life for which mechanical behavior becomes superior in air rises to higher stress levels as the oxidation tendency of the alloying element increases.

The changes created in the oxidation characteristics of the solvent metal also show the effect of the alloying elements. Judicious choice of solute element permits the formation of internal oxidation or dispersed oxide particles under proper conditions; thus, the material can be strengthened for elevated temperature use.

Summary

The high temperature mechanical behavior of nickel alloys under repeated stressing was investigated in air and argon atmospheres. Striking differences related to the environmental and solute element effects were found in the behaviors of these alloys.

The behavior in the air atmosphere under repeated stressing at 1500° F. (see Figure 5) was typical of fatigue-type behavior. This behavior indicated the strengthening effect of the alloying elements. Surface oxide, oxide blunting of crack tips, and internal oxidation, that is, dispersed oxide particles, produced under these testing conditions, were the primary strengthening mechanisms.

The material behavior in the argon atmosphere showed no differentiation in the endurance life in the alloys tested (see Figure 6). As no oxygen was present, the oxide strengthening mechanisms could not operate. The testing temperature was relatively high with respect to the melting point of pure nickel, approximately 0.63 T_{mp}; hence, solid solution alloying effects were negligible and creep-type behavior was the controlling mode.

For each alloy, a comparison of the mechanical behaviors in air and argon was made, Figures 8 to 11. In general, specimens tested in the inert argon atmosphere showed superior mechanical behavior at short endurance life, while those tested in air were superior at long endurance life. The range for which the behavior of the air-tested specimens is superior is qualitatively related to the relative tendency toward oxidation of the principal alloying element compared with the host metal, nickel.

Conclusions

The following conclusions can be obtained from the present study of the high temperature mechanical behavior of binary nickel alloys at 1500° F.

(1) In the oxidizing air atmosphere, the relative endurance life of the alloys can be qualitatively related to the 1500° F. tensile strengths.

(2) Tensile strength and fatigue strength are not related when repeated stressing occurs in an inert argon atmosphere at 1500° F. Analogous to creep at temperatures greater than one-half the absolute melting temperature, the endurance life is related primarily to the properties of the host material.

(3) In accord with the literature, three oxide strengthening mechanisms were found to operate under the oxidizing conditions employed. They are:

   (a) surface oxide inhibiting surface slip
   (b) oxide blunting of crack tips
   (c) internal oxidation.

(4) Significant increases of solute concentration along interior grain boundaries are caused primarily by oxidation. Subsequent decreases of solute in adjacent areas were also observed.

(5) Inert atmospheres are better for short service life, while oxidizing atmospheres are superior for longer life at 1500° F. The range in which the mechanical behavior in an oxidizing atmosphere is superior is qualitatively related to the ease of oxidation of the alloying element compared to that of the host material. These findings have potential value as guidelines for design of alloys for use under conditions involving repeated stress at at elevated temperatures.

Further Work

The following suggestions for further study are made with the purpose of guiding continued research in this area.

(1) Two adjustments with respect to equipment should be attempted. A smaller atmosphere chamber should be developed. This would facilitate simpler and more complete flushing. Secondly, the method of temperature sensing and control should be reevaluated with respect to precision and accuracy.

(2) A series of tests similar to that in the present work but at an intermediate temperature would be enlightening. In this series, the combination of both intergranular and transgranular fracture could be examined.

(3) Another approach could be a study involving a single binary alloy in the following types of atmospheres:

(a) oxidizing to both solvent and solute elements

(b) oxidizing to solute element only

(c) non-oxidizing, i.e. inert, with respect to the entire alloy.

This study would provide for a more complete evaluation of the effects of oxide formation and dispersed oxides.

Further Work

The following suggestions for further study are made with the purpose of guiding continued research in this area.

(1) Two adjustments with respect to equipment should be attempted. A smaller atmosphere chamber should be developed. This would facilitate simpler and more complete flushing. Secondly, the method of temperature sensing and control should be reevaluated with respect to precision and accuracy.

(2) A series of tests similar to that in the present work but at an intermediate temperature would be enlightening. In this series, the combination of both intergranular and transgranular fracture could be examined.

(3) Another approach could be a study involving a single binary alloy in the following types of atmospheres:

(a) oxidizing to both solvent and solute elements

(b) oxidizing to solute element only

(c) non-oxidizing, i.e. inert, with respect to the entire alloy.

This study would provide for a more complete evaluation of the effects of oxide formation and dispersed oxides.

Appendix I Stress Calculation

Stresses at the surface of the specimens were calculated using the flexure formula obtained from Popov (50). This equation

$$S_{max} = \frac{Mc}{I}$$

where S_{max} = maximum stress

M = bending moment

c = distance from neutral axis to surface

I = centroidal moment of inertia

can be rewritten, when appropriate substitutions are made, as

$$S_{max} = \frac{19.5\ P}{wt^2}$$

where P = applied load

w = width of specimen at reduced section

t = specimen thickness.

Bibliography

1. Cottrell, A. H. and Hull, D., "Extrusion and Intrusion by Cyclic Slip in Copper", Royal Society, Proceedings, series A, vol. 242, (1957), p. 211.

2. Machlin, E. S., "Dislocation Theory of the Fatigue of Metals", National Advisory Committee for Aeronautics, Technical Note #1489, (1948).

3. Machlin, E. S., "An Application of Dislocation Theory to Fracturing by Fatigue" from Fracturing of Metals, American Society for Metals, Cleveland, (1952), p. 282.

4. Wood, W. A., "Mechanism of Fatigue" from Fatigue in Aircraft Structure, ed. Freudenthal, A. M., New York: Academic Press, (1956), p. 1.

5. Parker, E. R., "Theories of Fatigue" from Mechanical Properties of Materials at Elevated Temperatures, New York: McGraw-Hill, (1961), p. 129.

6. Weber, J. H., "Observations on the Fracture Mode and Fatigue Life of Type 304 Stainless Steel at Elevated Temperatures", Undergraduate Thesis, Lehigh University, (1963).

7. Meleka, A. H., "Combined Creep and Fatigue Properties", Metallurgical Reviews, v. 7, #25, (1962), p. 43.

8. Kennedy, A. J., "Effect of Fatigue Stresses on Creep and Recovery" from Proceedings, International Conference on Fatigue of Metals, London: Institution of Mechanical Engineers, (1956), p. 401.

9. Gilbert, P. T., "Corrosion Fatigue", Metallurgical Reviews, v. 1, (1956), p. 379.

10. McKay, R. J. and Worthington, R., Corrosion Resistance in Metals and Alloys, New York: Reinhold Pub. Co., (1956).

11. Wolf, J. S., Weeton, J. W., and Freche, J. F., "Observations of Internal Oxidation in Six Nickel-Base Alloy Systems", NASA Technical Note D-2813, (1965).

12. Harper, D. L., Feilbach, W. H., and Libsch, J. F., "Application of Induction Heating to High Temperature Fatigue Testing", ASTM Proceedings, v. 63, (1963), p. 684.

13. Feilbach, W. H., "Capabilities of New Equipment for High Temperature Fatigue Testing with Thermal Pulsing",

M. S. Thesis, Lehigh University, (1963).

14. Teeple, H. O., "Nickel and High-Nickel Alloys", Industrial and Engineering Chemistry, v. 46, (1954), p. 2092.

15. Forrest, P. G., "Influence of Temperature on Fatigue Strength", from Chapter VIII of Fatigue of Metals, New York: Pergamon Press, (1962) p. 238.

16. Harper, D. L., "Application of Induction Heating to High Temperature Fatigue Testing", M. S. Thesis, Lehigh University, (1962).

17. Dunsby, J. A., "On the Furnace Requirements for the Mechanical Testing of Materials at Elevated Temperatures", Mechanical Engineering Report MS-103, N.R.C. #6073, Ottawa, (1960).

18. Daniels, D. J. and Hall, A. M., "Nickel and Its Alloys" from Reactors Handbook, v. I, (1960), p. 636.

19. Lozinskiy, M. G. and Pertsovskiy, N. Z., "High-Temperature Fracture Mechanism of Polycrystalline Metals", Fiz. Metal. Metalloved., v. 17, no. 6, (1964), p. 903.

20. Basquin, "The Exponential Law of Endurance Tests", ASTM, Proceedings, v. 10, (1910), p. 625.

21. Garofalo, F., Fundamentals of Creep and Creep-Rupture in Metals, New York: Macmillan, (1965).

22. Dennison, J. P., Llewellyn, R. J., and Wilshire, B., "The Creep and Fracture Behavior of Some Dilute Nickel Alloys at 500 and 600 °C", Journal of the Institute of Metals, v. 94, no. 4 (1966), p. 130.

23. Danek, G. J., Smith, H. H., and Achter, M. R., "High-Temperature Fatigue and Bending Strain Measurements in Controlled Environments", ASTM Proceedings, v. 61, (1961), p. 775.

24. Achter, M. R. and Fox, H. W., "The Effect of Surface Adsorption of Gas on Crack Propagation", AIME, Transactions, v. 215, (1959), p. 295.

25. Cass, J. R., and Achter, M. R., "Oxide Bonding and the Creep-Rupture Strength of Nickel", AIME, Transactions, v. 224, (1962), p. 1115.

26. Coughlin, J. P., "Contributions to the Data on Theoretical Metallurgy - XII. Heats and Free Energies of Formation

of Inorganic Oxides", U. S. Bureau of Mines, Bulletin no. 542, (1954).

27. Swalin, R. A. and Martin, A., "Diffusion of Magnesium, Silicon, and Molybdenum in Nickel", AIME, Transactions, v. 209, (1957), p. 936.

28. Achter, M. R. and Shahinian, P., "A Comparison of the Creep-Rupture Properties of Nickel in Air and Vacuum", AIME, Transactions, v. 215, (1959), p. 37.

29. Allen, J. M., "Environmental Factors Influencing Metal Applications in S pace Vehicles", DMIC Report #142, Columbus, Ohio: Battelle Memorial Institute, (1960).

30. Swanson, H. E. and Tatge, E., "Standard X-ray Diffraction Powder Patterns", U. S. National Bureau of Standards Circular no. 539, v. 1, (1953).

31. Frendenthal, A. M., "Aspects of Fatigue Damage Accumulation at Elevated Temperatures", Acta Met., v. 11, no. 7, (1963), p. 753.

32. McEvily, A. J. and Boettner, R. C., "On Fatigue Crack Propagation in F.C.C. Metals", Acta Met., v. 11, no. 7, (1963), p. 725.

33. McHenry, H. J. and Probst, H. B., "Effects of Environments of NaOH, Air, and Argon on the Stress-Rupture Properties of Nickel at 1500°F", NACA Tech. Note 3987, (1958).

34. Stegman, R. L. and Achter, M. R., "Effect of Temperature on Nickel Fatigued in Vacuum", ASM Transactions, v. 57, (1964), p. 603.

35. Ronay, M., Reimann , W. H., and Wood, W. A., "Mechanism of Fatigue Deformation at Elevated Temperatures", AIME, Transactions, v. 233, (1965), p. 298.

36. Alden, J. H., "Fatigue Fracture in Pure Metals", Journal of Metals, v. 14, no. 11, (1962), p. 828.

37. Clark, F. H., "Scaling", Chapter 11 from Metals at High Temperatures, New York: Reinhold, (1950), p. 339.

38. Doerr, R. M., "High Temperature Corrosion Studies - Nickel and Cobalt in Air and Oxygen", U. S. Bureau of Mines, Report of Investigations no. 6231, (1963).

39. Gulbransen, E. A. and Andrew, K. F., "The Kinetics of Oxidation of High Purity Nickel", Journal, Electrochem.

Soc., v. 101, (1954), p. 128.

40. Tylecote, R. F., "Factors Influencing the Adherence of Oxides on Metals", J.I.S.I., v. 196, (1960), p. 135.

41. Sartell, J. A. and Li, C. H., "The Mechanism of Oxidation of High Purity Nickel in the Range 950-1200°C", Journal, Institute of Metals, v. 90, (1961), p. 92.

42. Mullendove, A. W. and Grant, N. J., "Grain Boundary Behavior in High Temperature Deformation and Fracture" from Mechanisms Operating in Metals at Elevated Temperatures, (1961), p. 151.

43. Lazan, B. J., "Fatigue of Structural Materials at High Temperature", High Temperature Effects in Aircraft Structures, New York: Pergamon Press, (1958), p. 171.

44. Gulbransen, E. A. and Andrew, K. F., "High-Temperature Oxidation of High Purity Nickel between 750° and 1050°C", Journal, Electrochem. Soc., v. 104, (1957), p. 451.

45. Shim, M. J. and Moore, W. J., "Diffusion of Nickel in Nickel Oxide", J. Chem. Phys., v. 26, (1957), p. 802.

46. Keith, R. E., Siebert, C. A., and Sinnott, M. J., "An Investigation of Intergranular Oxidation in Type 310 Stainless Steel", Symposium on Basic Effects of Environment on Strength, Scaling and Embrittlement of Metals at High Temperatures, ASTM, Special Technical Publication 171, (1955), p. 49.

47. Pillings and Bedworth, "The Oxidation of Metals at High Temperatures", Journal, Institute of Metals, v. 29, (1923), p. 529.

48. Allison, H. W. and Samelson, H., "Diffusion of Aluminum, Magnesium, Silicon, and Zirconium in Nickel", Journal Appl. Phys., v. 30, (1959), p. 1419.

49. Swalin, R. A. and Martin, A., "Solute Diffusion in Nickel-base Substitutional Solid Solutions", AIME, Transactions, v. 206, (1956), p. 567.

50. Popov, E. P., Mechanics of Materials, Englewood Cliffs, New Jersey: Prentice Hall, (1952), p. 100.

Table I

Chemical Composition of Alloys - Weight Percent

Element	Pure Nickel	Nickel-aluminum	Nickel-beryllium	Nickel-silicon
Carbon	0.008	0.006	0.018	0.018
Aluminum	0.014	2.44 (5.16)[1]	0.017	0.011
Silicon	0.038	0.011	0.018	2.63 (5.35)
Beryllium	-[2]	-	0.94 (5.78)	-
Nickel	Bal.	Bal.	Bal.	Bal.
Molybdenum	-	-	-	-
Chromium	0.0024	0.0016	0.0019	0.0019
Cobalt	0.039	0.040	0.052	0.036
Titanium	0.0043	0.0045	0.0040	0.0098
Iron	0.023	0.024	0.13	0.60
Manganese	0.051	0.076	0.010	0.45
Phosphorus	<0.001	<0.001	<0.0018	<0.001
Sulfur[3]	8	<1	<1	4
Arsenic	-	-	-	-
Antimony	<0.001	<0.001	<0.001	<0.001
Lead	<0.001	<0.001	<0.01	<0.01
Tin	-	-	-	-

Notes:

(1) figure in parentheses denotes atomic percentage

(2) dash denotes element not detected

(3) element given in parts per million

Table II

Tensile Test Data

A. Room Temperature Test Data

Alloy	0.2% Yield Strength (psi)	Ultimate Tensile Strength (psi)
Pure Ni	8,230	47,300
	8,500[1]	46,000[1]
Ni-Al	16,750	58,825
Ni-Si	20,010	68,850
Ni-Be	22,035	81,225

B. 1500° F. Test Data

Alloy	0.2% Yield Strength (psi)	Ultimate Tensile Strength (psi)
Pure Ni	4,200	6,025
Ni-Al	6,620	13,275
Ni-Si	6,920	10,975
Ni-Be	9,945	17,455[2]

Notes:

(1) from Daniels and Hall, Reference 18.

(2) no failure occurred.

Table III

X-ray Diffraction Data

	Base material		Oxide		
Alloy	Structure	a_o(Å)	Structure	Oxide	a_o(Å)
Pure Ni	f.c.c.	3.529	f.c.c. (NaCl)[1]	NiO	4.194
		3.5238[2]			4.1946[3]
Ni-Al	f.c.c.	3.542	f.c.c. (NaCl)	(Ni,Al)O	4.198
Ni-Si	f.c.c.	3.528	f.c.c. (NaCl)	(Ni,Si)O	4.192
Ni-Be	f.c.c.	3.513	f.c.c. (NaCl)	(Ni,Be)O	4.188
	f.c.c.[4]	3.527[4]			

Notes:

(1) (NaCl) denotes oxide lattice structure type

(2) from Swanson and Tatge, Reference 30.

(3) from Gulbransen and Andrew, Reference 39.

(4) see discussion for explanation of this data

Table IV

Substrate Cracking Behavior

Alloy	Atmosphere	Stress[1]	Life[2]	Number of cracks[3]	Branching[4]
Pure Ni	air	4,000	10^7	many	-
		8,000	10^4	many (D)	yes
	argon	3,000	10^7	many	-
		10,000	10^5	many (D)	yes
Ni-Al	air	6,500	10^7	many	-
		10,000	10^5	few (B)	yes
	argon	3,000	10^7	one (A)	-
		13,000	$3x10^4$	several (C)	yes
Ni-Be	air	7,000	10^7	many	-
		12,000	$2x10^4$	few (B)	yes
	argon	3,000	10^7	very few	-
		14,000	$2x10^4$	several (C)	yes
Ni-Si	air	5,500	10^7	many	-
		11,000	$3x10^4$	one	yes
	argon	4,000	10^7	one (A)	-
		13,000	$3x10^4$	several (C)	yes

Notes:

(1) approximate stress level (psi) of testing of specimens observed

(2) order of magnitude of endurance life of specimens observed

(3) letters in parentheses designate a schematic photograph from from the following page

(4) designates presence or absence of branching

Table IV (cont'd.)

Schematic Photographs of Cracking Behavior

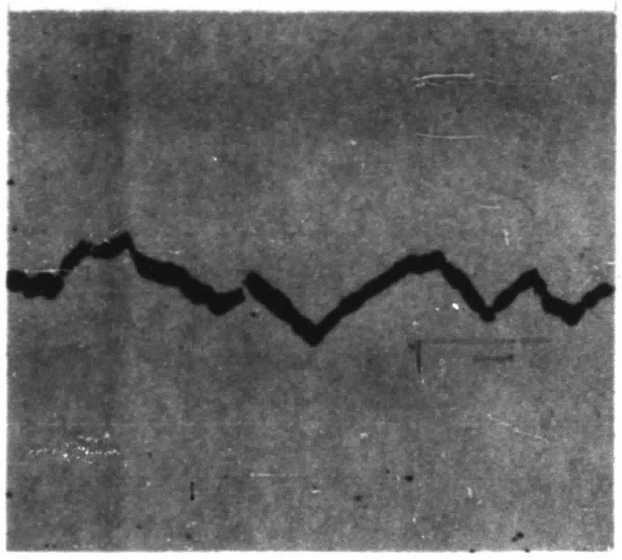

(A) One crack with no branching.

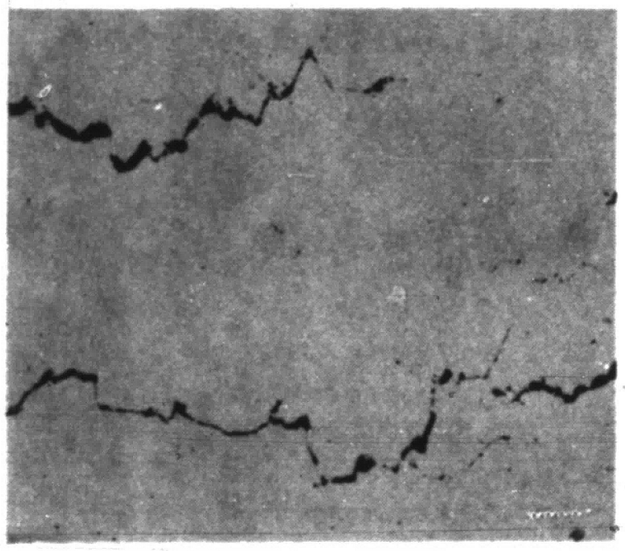

(B) A few cracks showing a slight amount of branching.

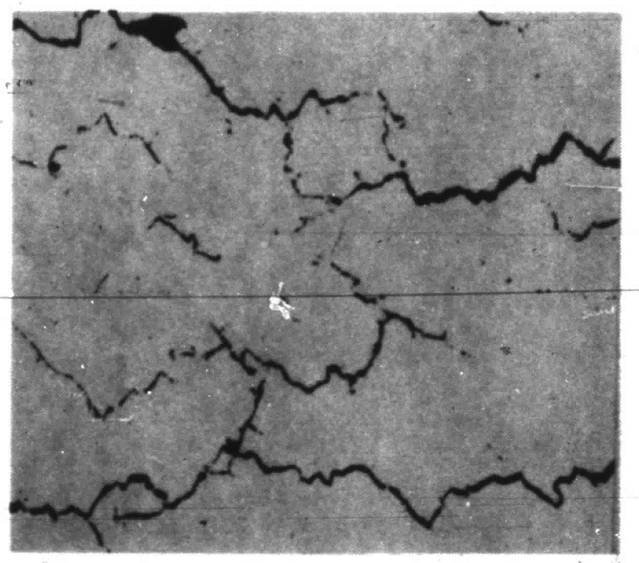

(C) Several cracks exhibiting numerous branches.

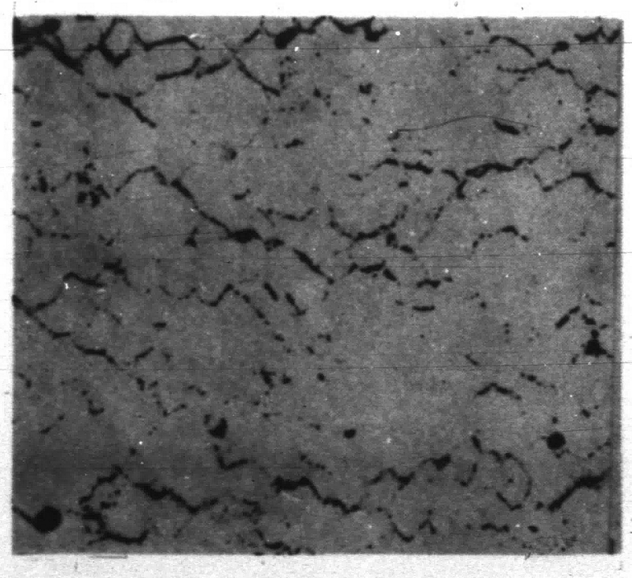

(D) Many cracks showing branching around many grains.

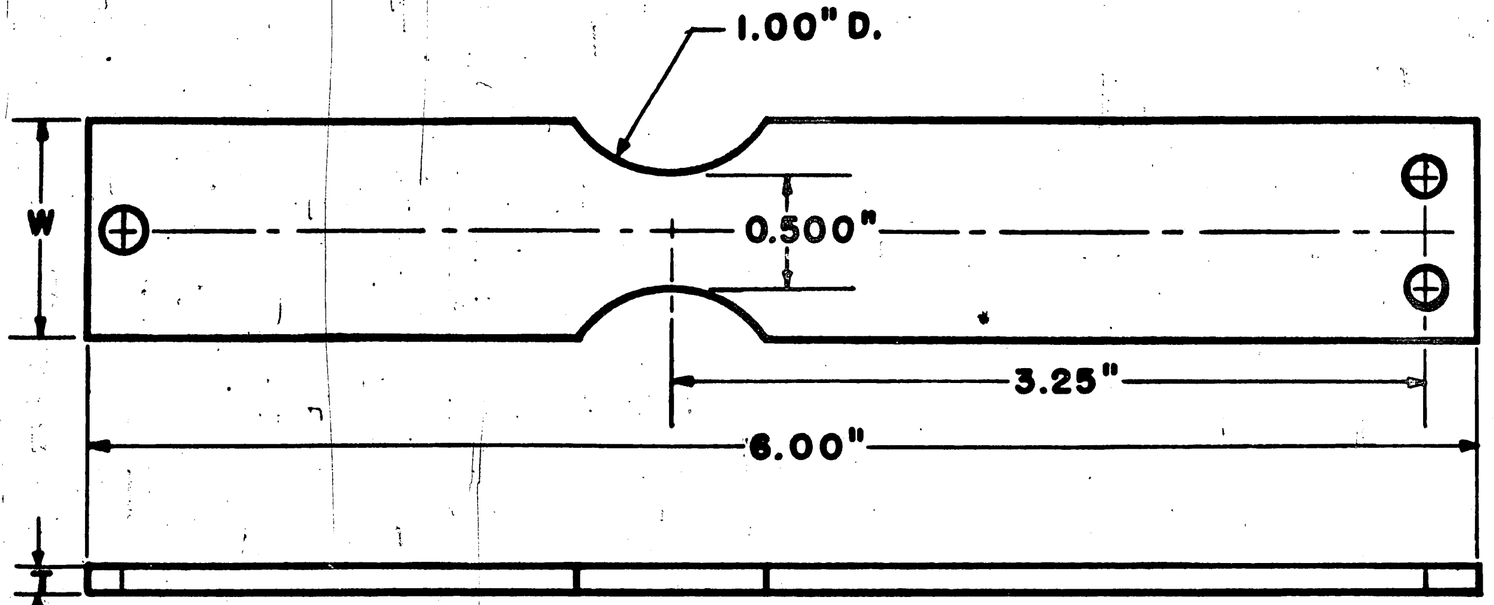

Figure 1 Fatigue specimen

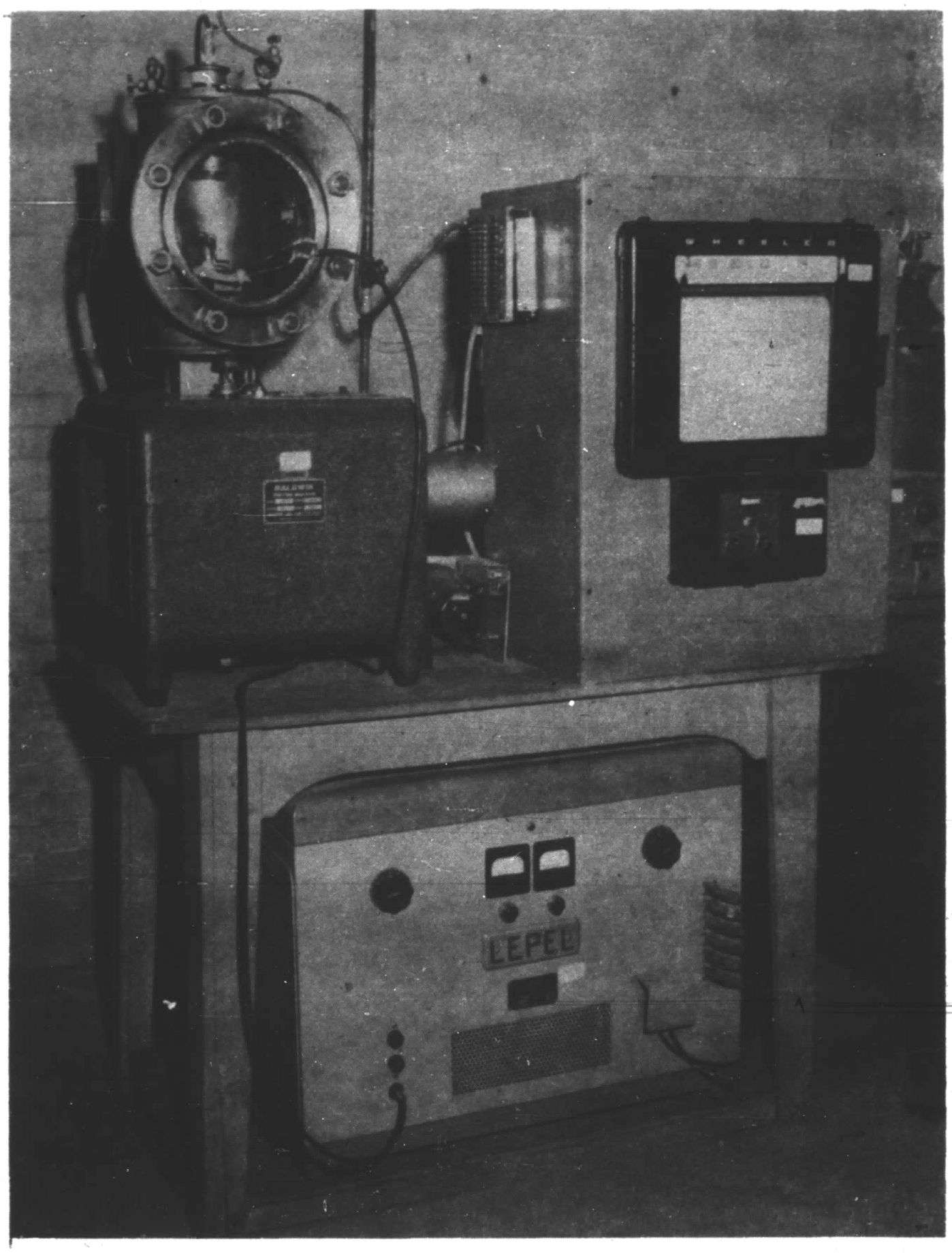

Figure 2 Fatigue testing equipment

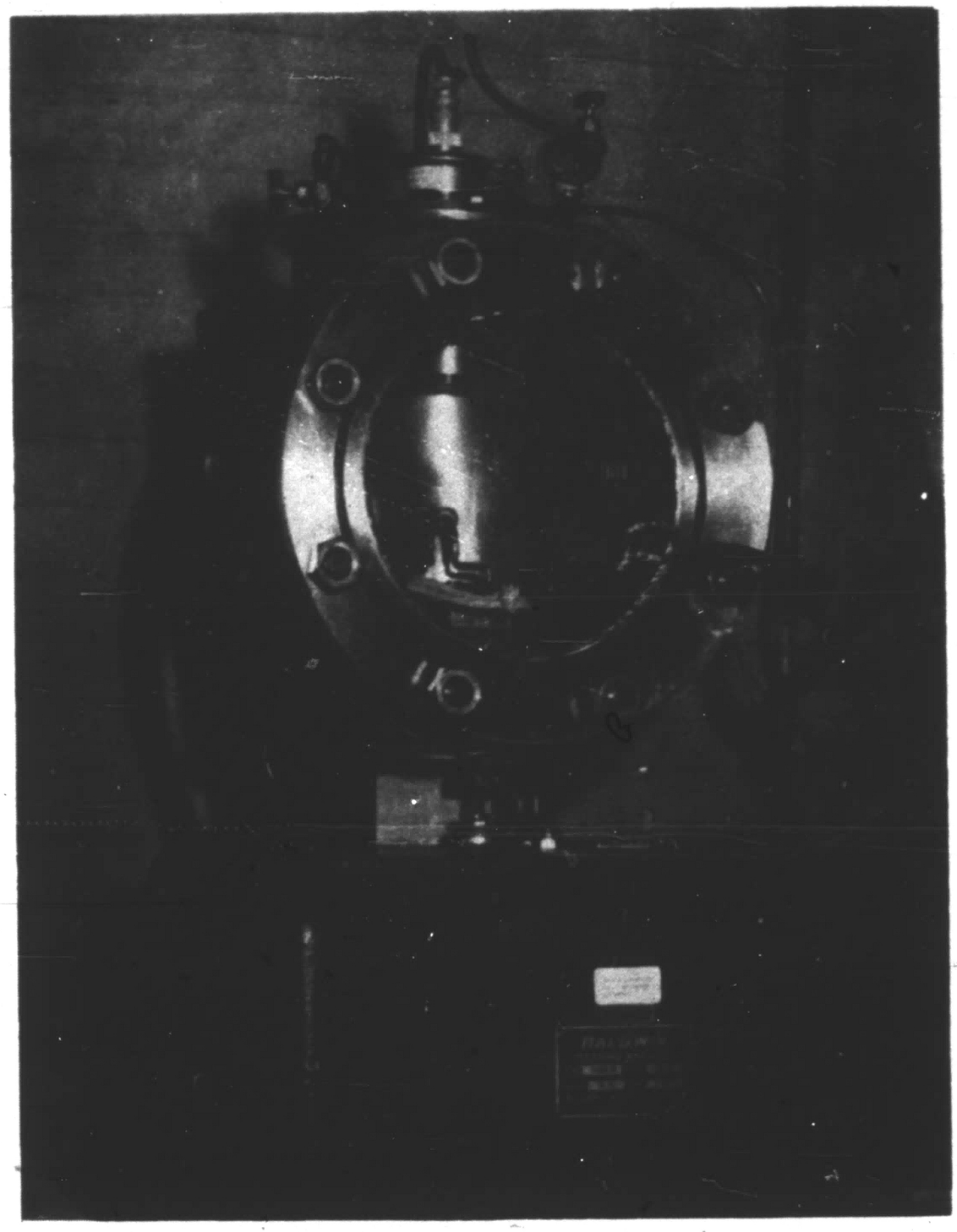

Figure 3 Atmosphere test chamber

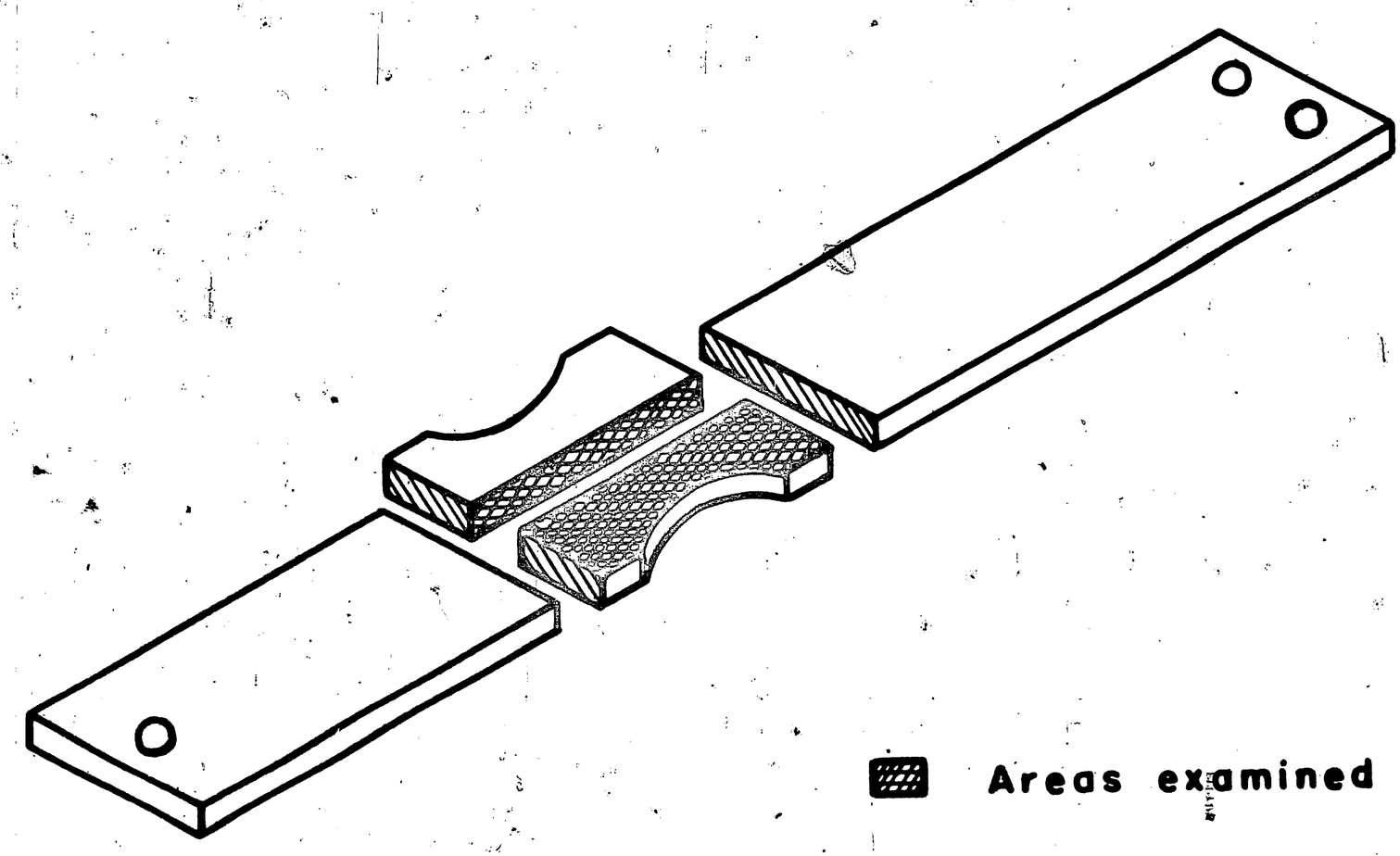

Figure 4 Sectioning for metallography

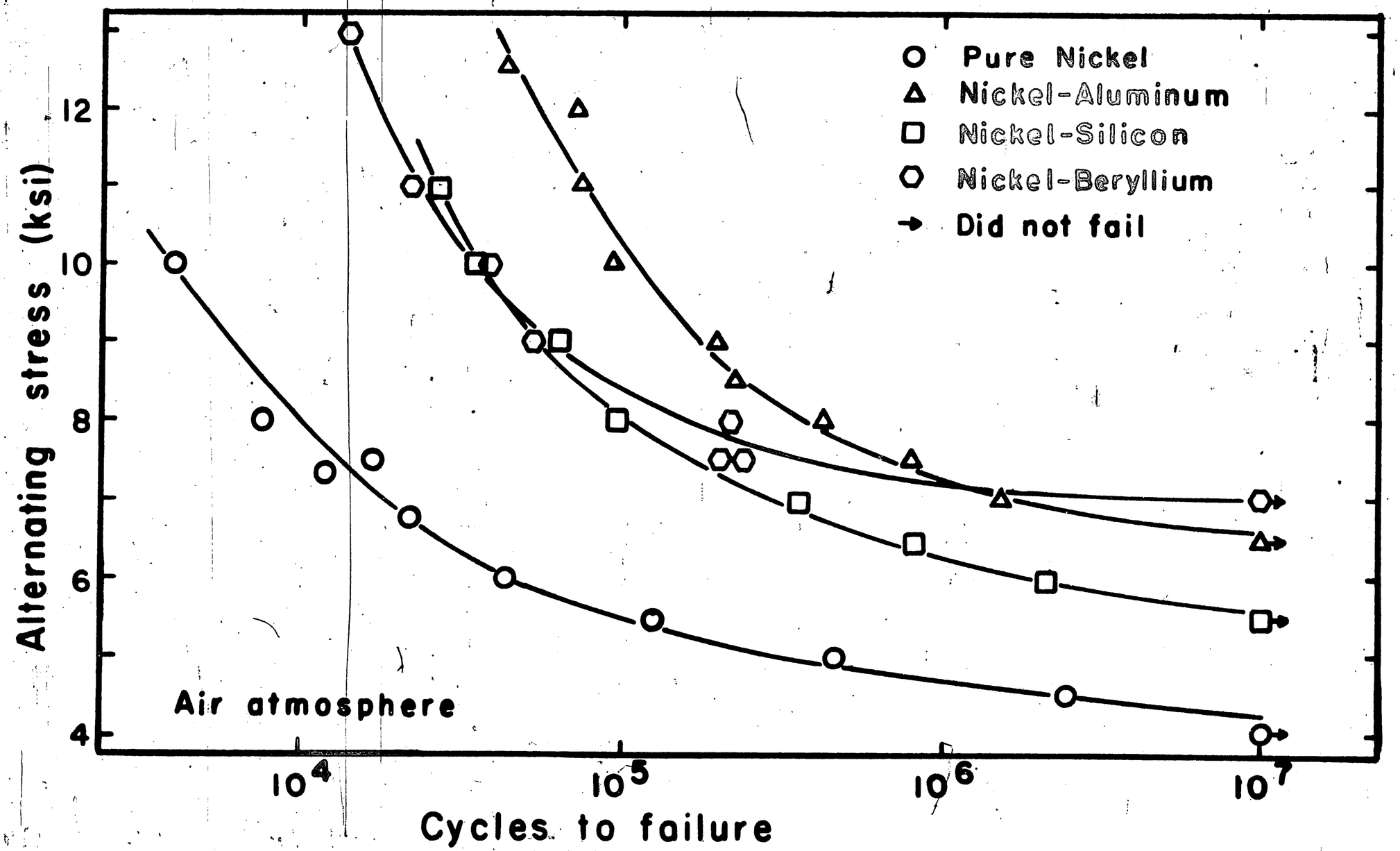

Figure 5 Fatigue data for nickel alloys tested in air at 1500° F.

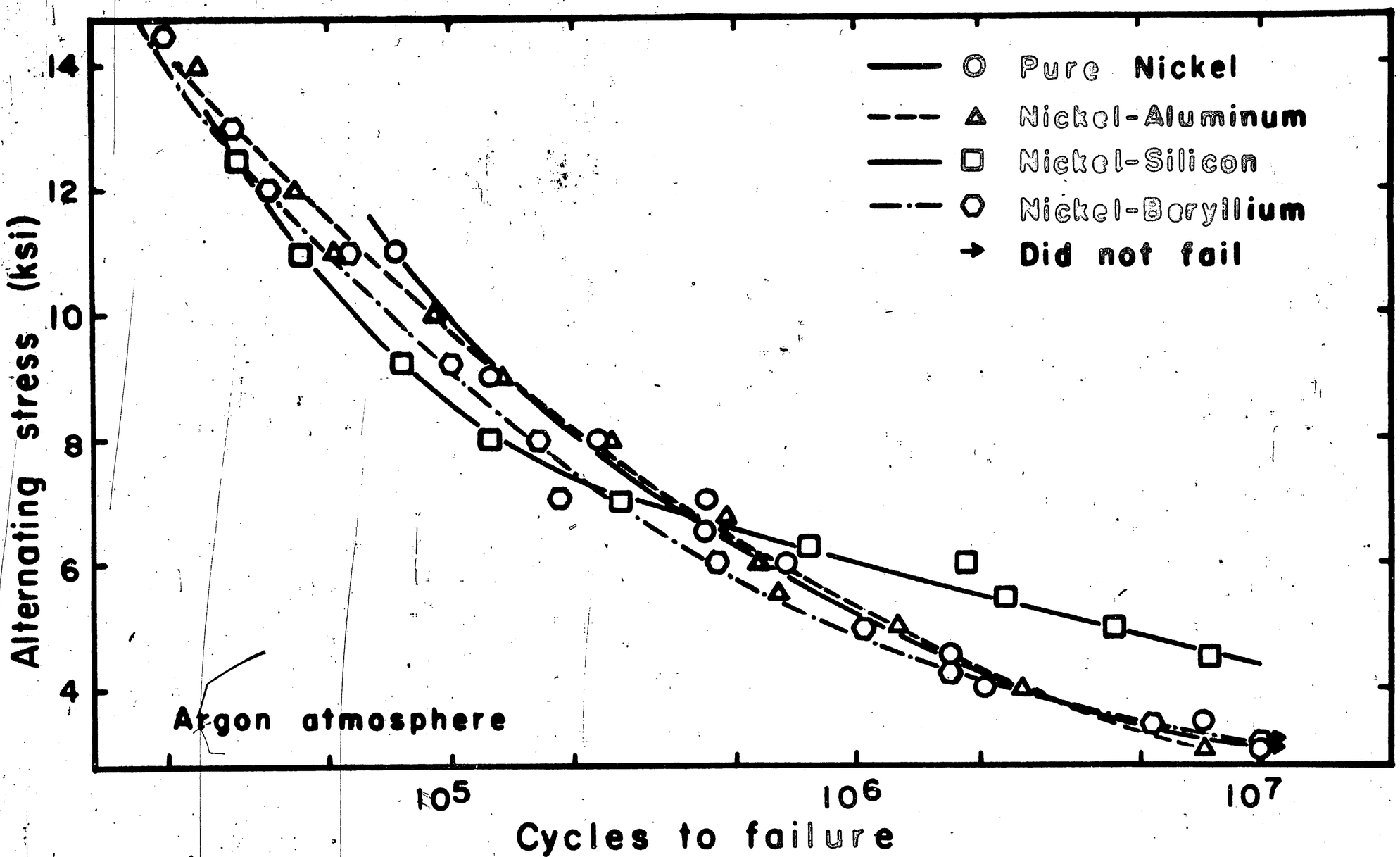

Figure 6 Fatigue data for nickel alloys tested in argon at 1500° F.

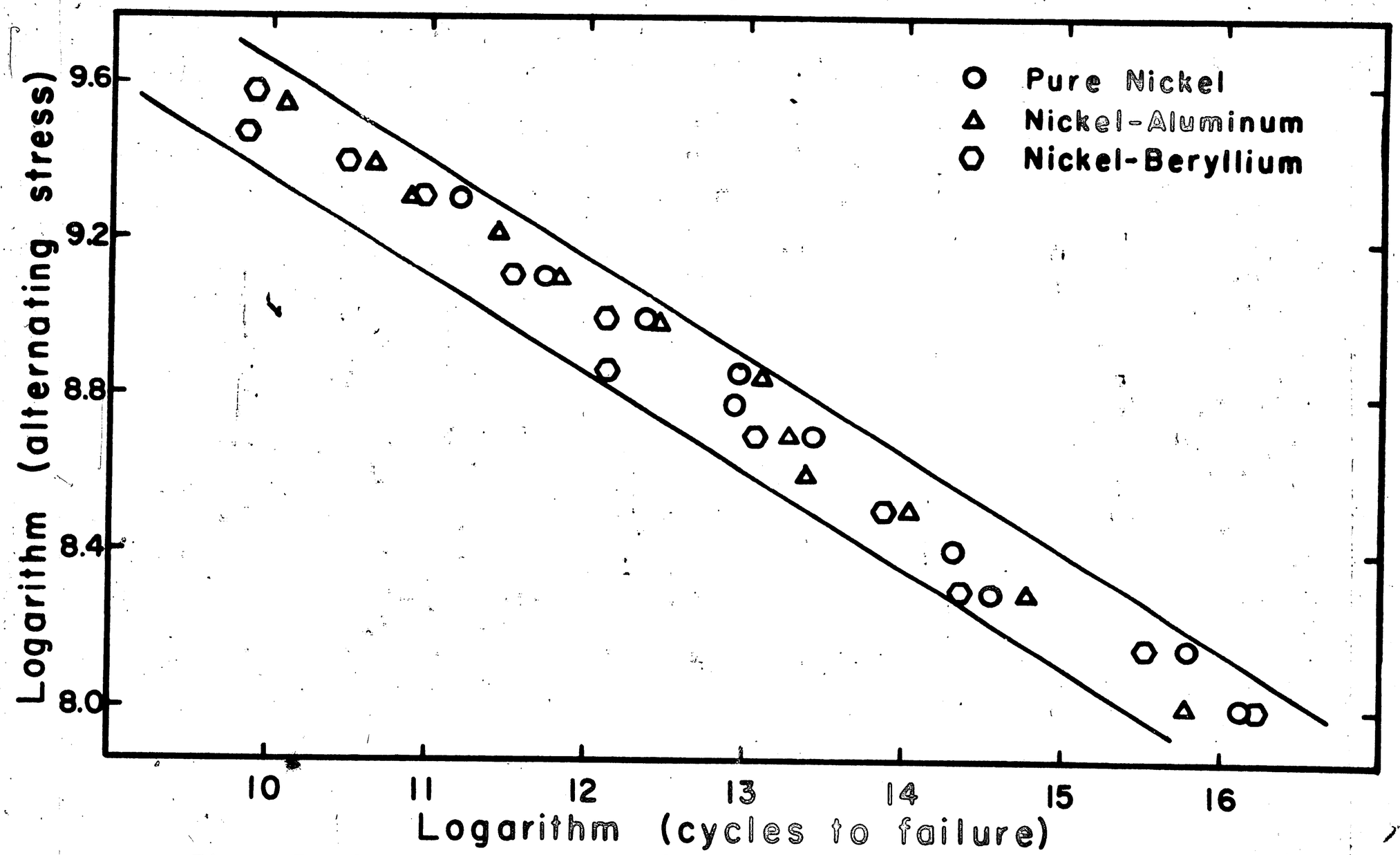

Figure 7 Stress vs. cycles to failure for pure nickel, Ni-Al, Ni-Be, alloys tested in argon at 1500° F.

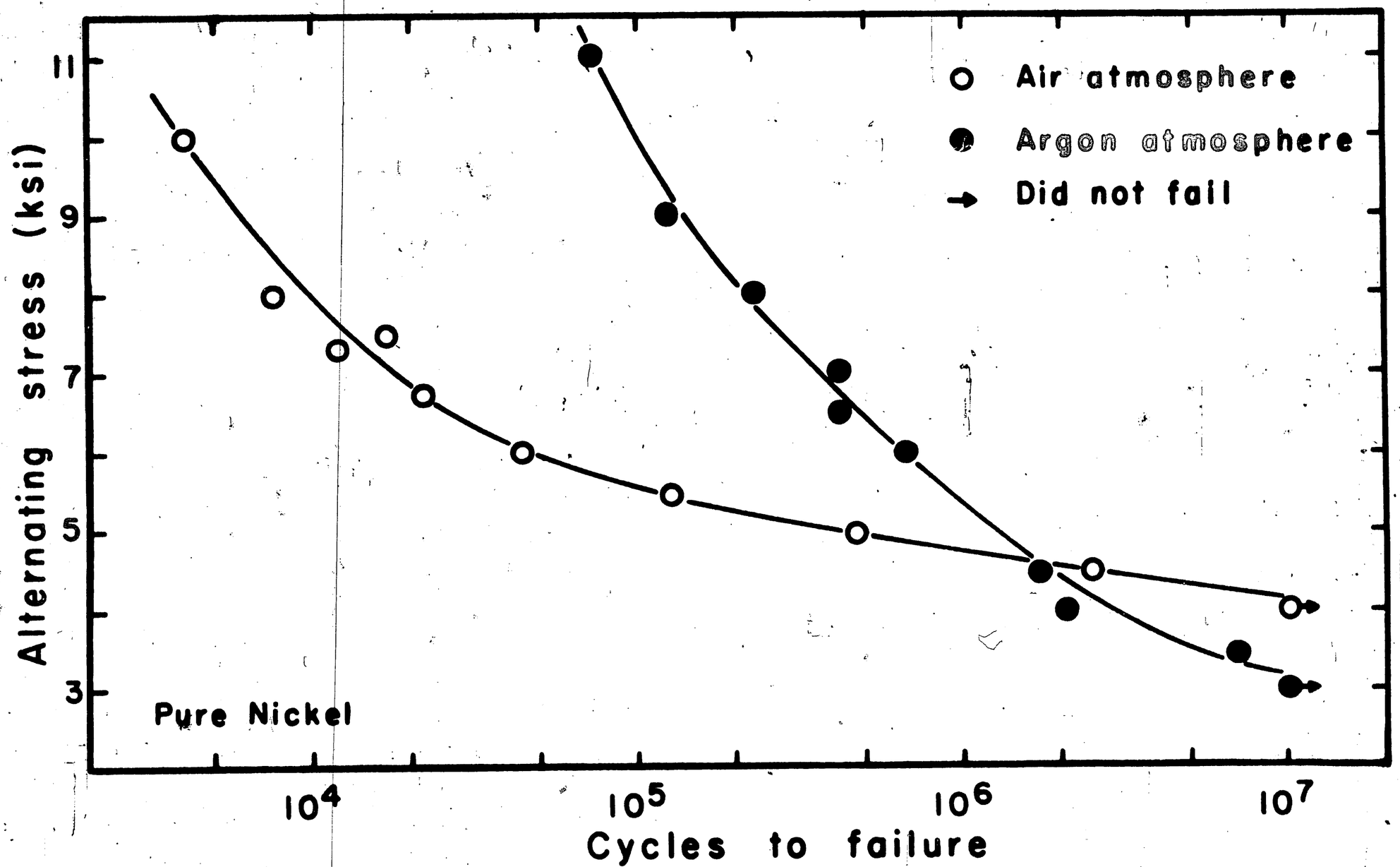

Figure 8 Comparison of fatigue behavior of pure nickel tested in air and in argon at 1500° F.

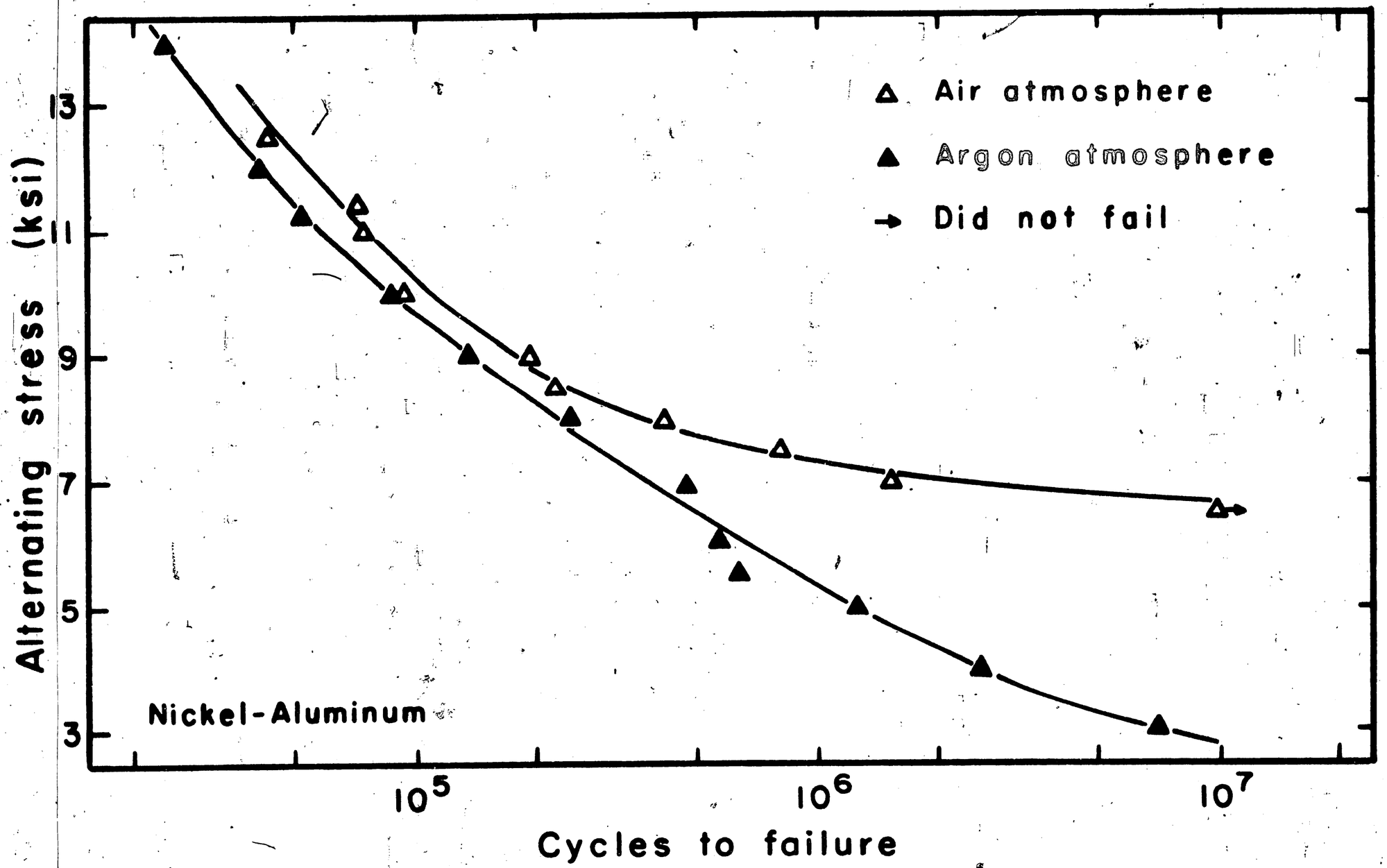

Figure 9 Comparison of fatigue behavior of Ni-Al alloy as tested in air and in argon at 1500° F.

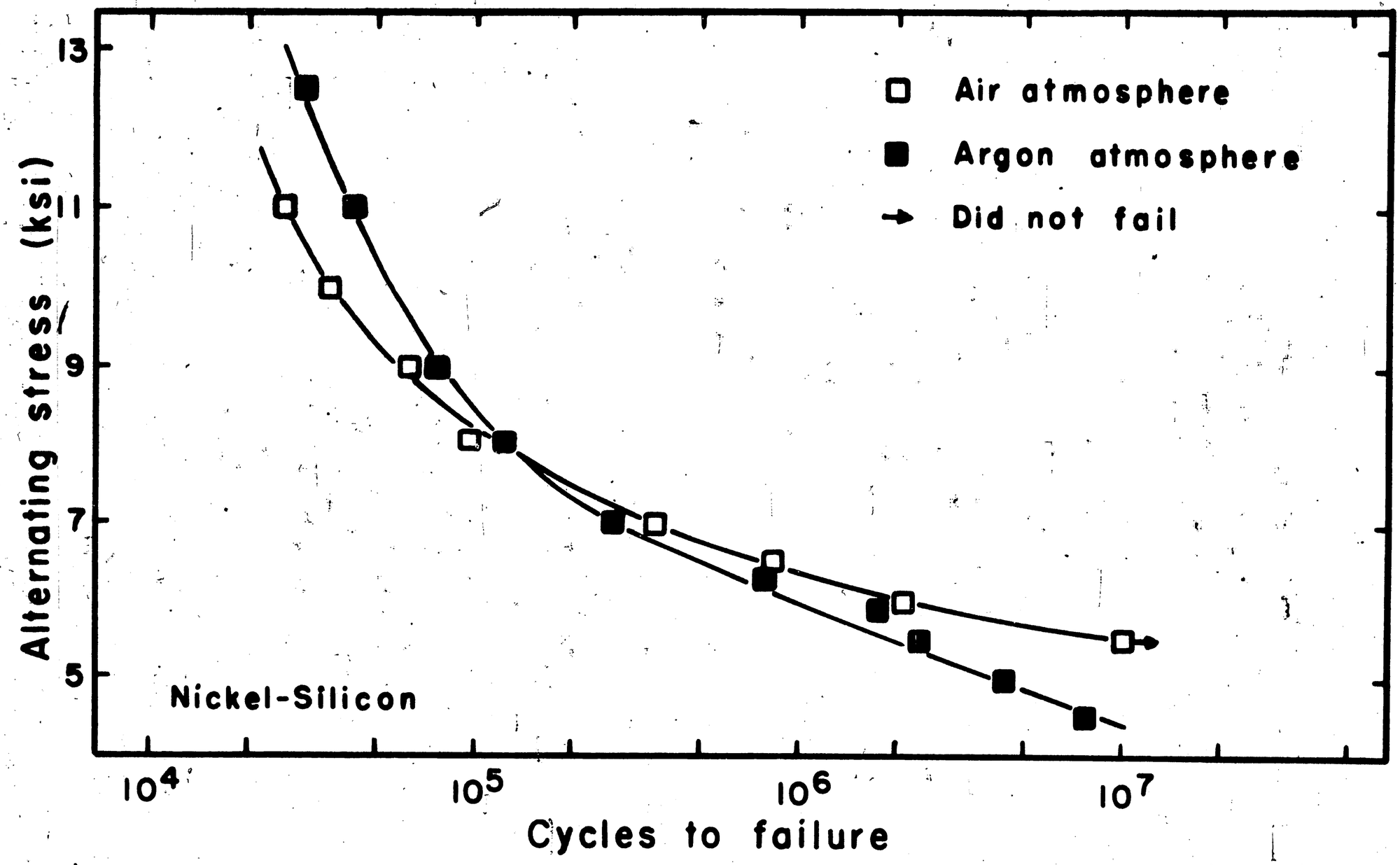

Figure 10 Comparison of fatigue behavior of Ni-Si alloy as tested in air and in argon at 1500° F.

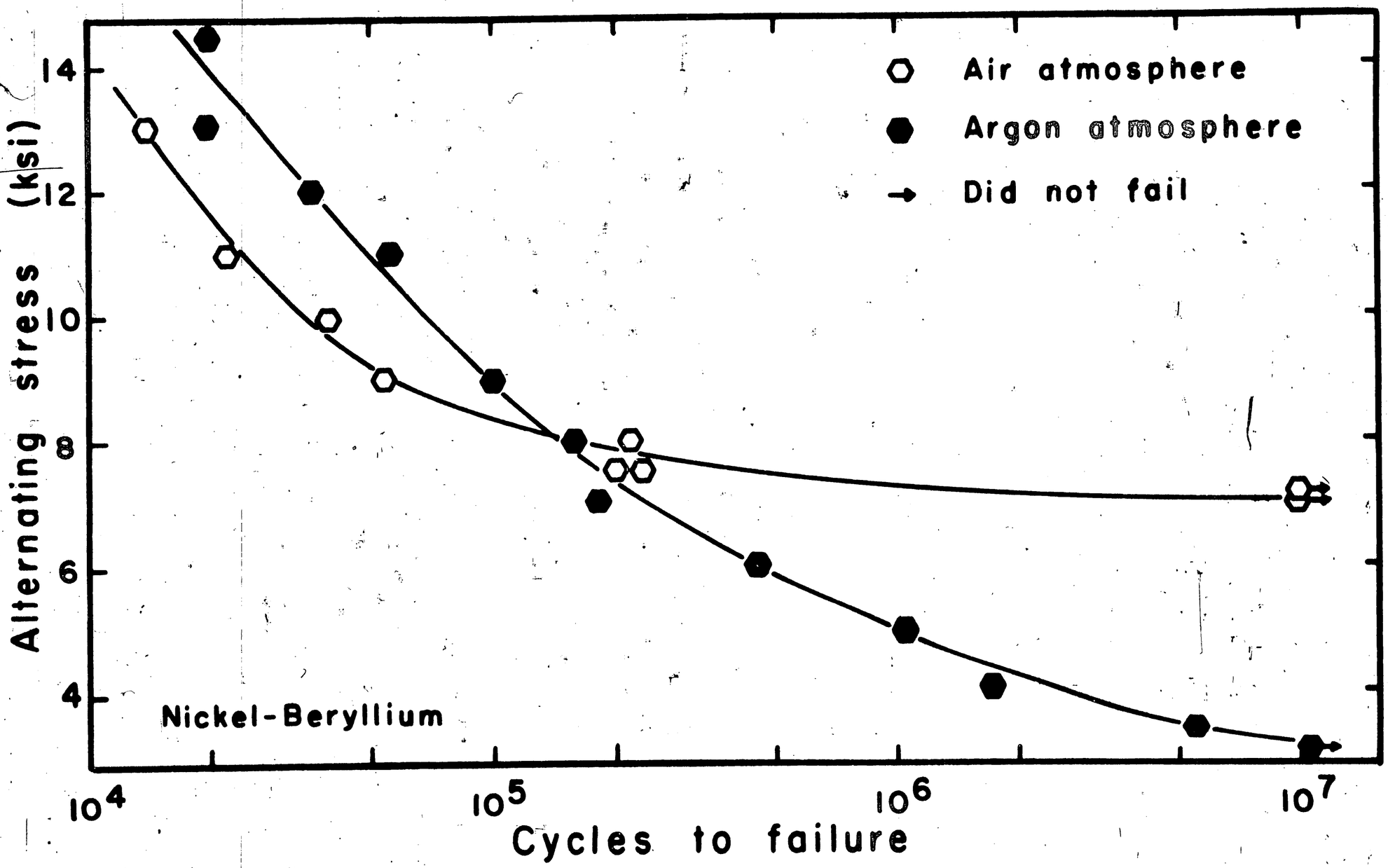

Figure 11 Comparison of fatigue behavior of Ni-Be alloy as tested in air and in argon at 1500° F.

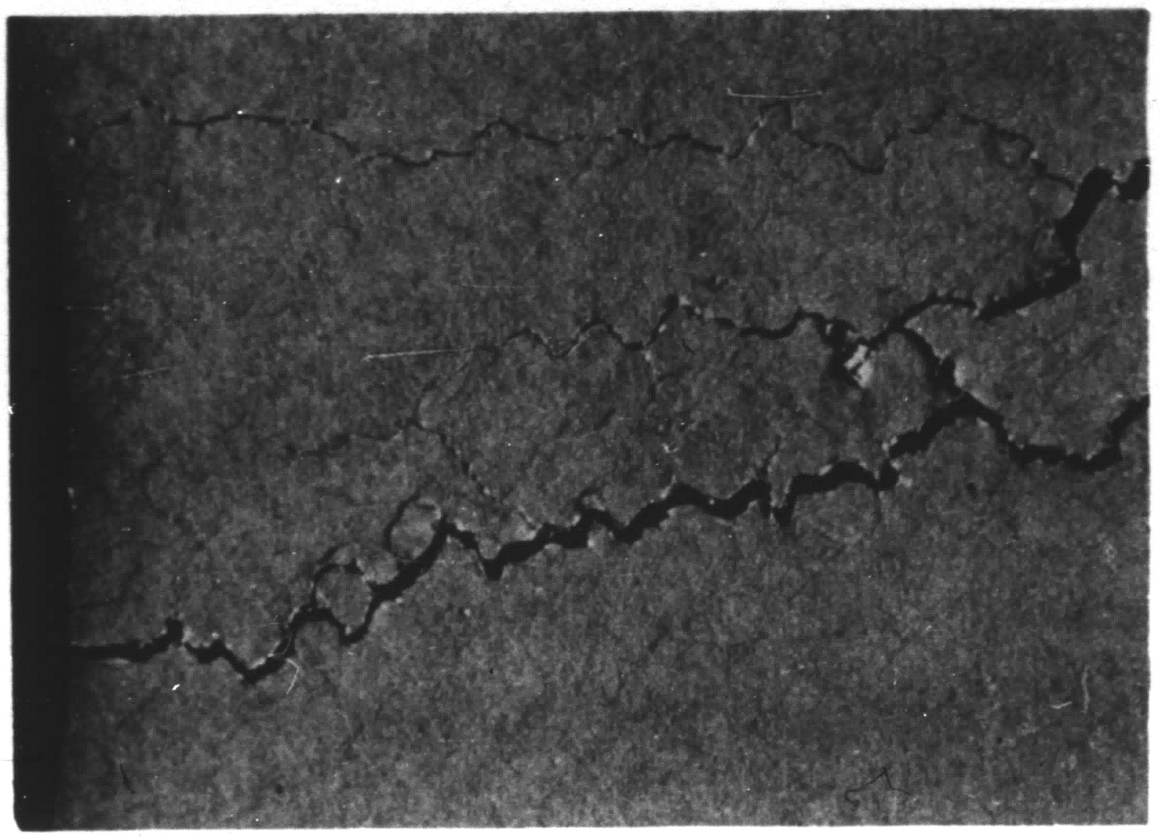

Figure 12 Macrograph of Ni-Be alloy showing typical surface view of fracture as tested in air (3.9×10^4 cycles), 15X.

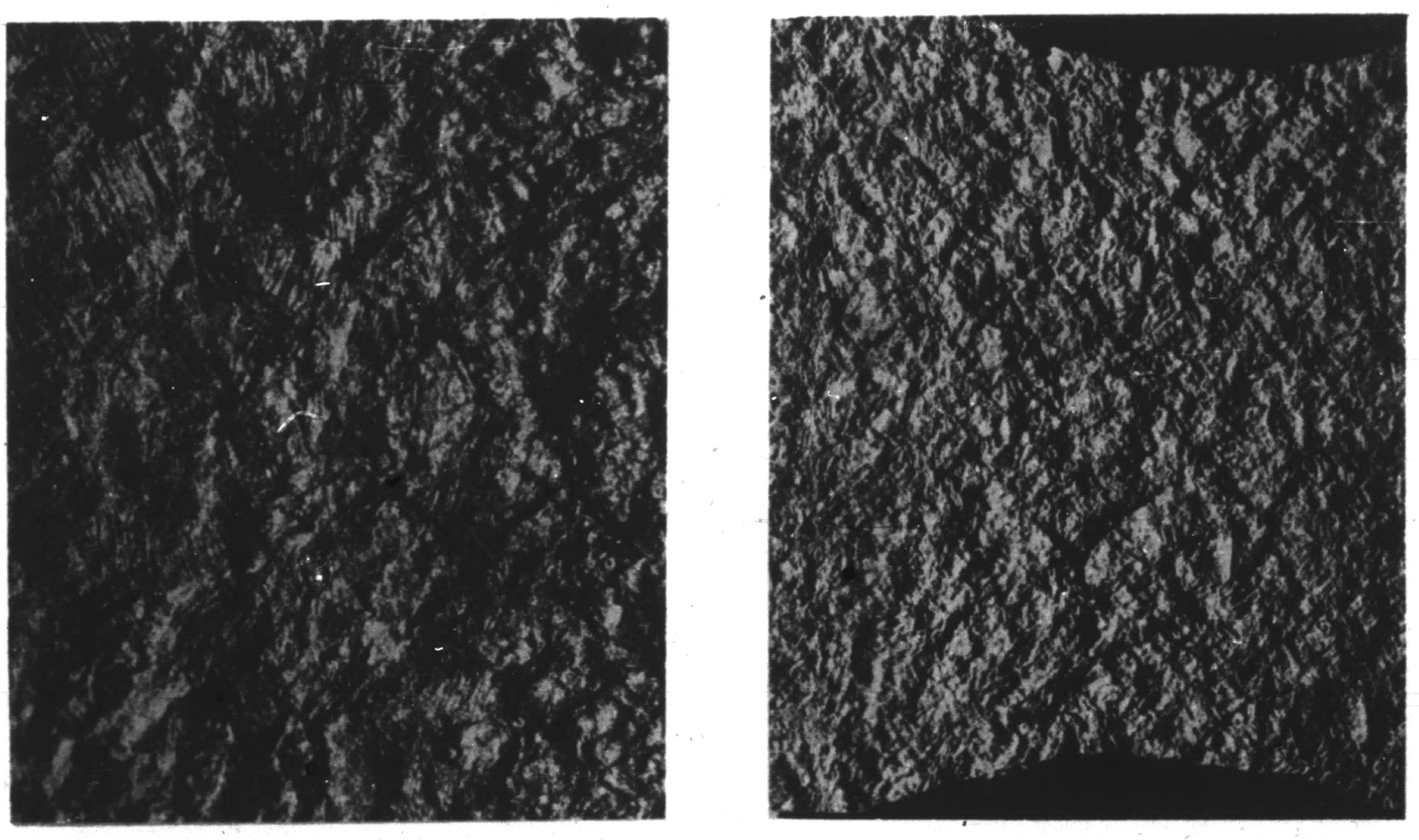

(a) (b)

Figure 13 Macrographs of pure nickel tested in argon (1.23×10^5 cycles. (a) surface slip in the grains, 14X, (b) surface roughness after testing, 5.2X.

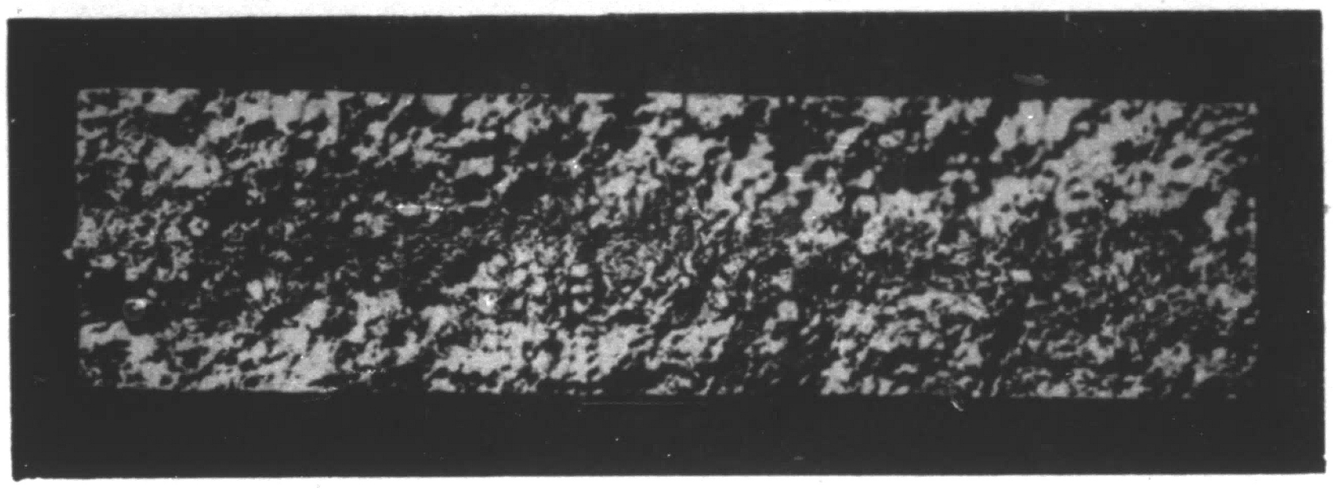

Figure 14. Macrograph of Ni-Si alloy tested in air (8.19×10^5 cycles) showing typical intergranular fracture surface, 8X.

Figure 15. Macrograph of pure nickel tested in air (7.5×10^3 cycles) showing fracture of oxide layer, 14X.

Figure 16 Macrograph of Ni-Be alloy tested in air (1.01×10^7 cycles) exhibiting flaking of oxide layer, 12X.

(a) (b)

Figure 17 Blunting of crack tips by oxide. (a) Pure nickel tested in air (1.02×10^7 cycles), 200X, (b) Ni-Be alloy tested in air (1.0×10^7 cycles), 250X.

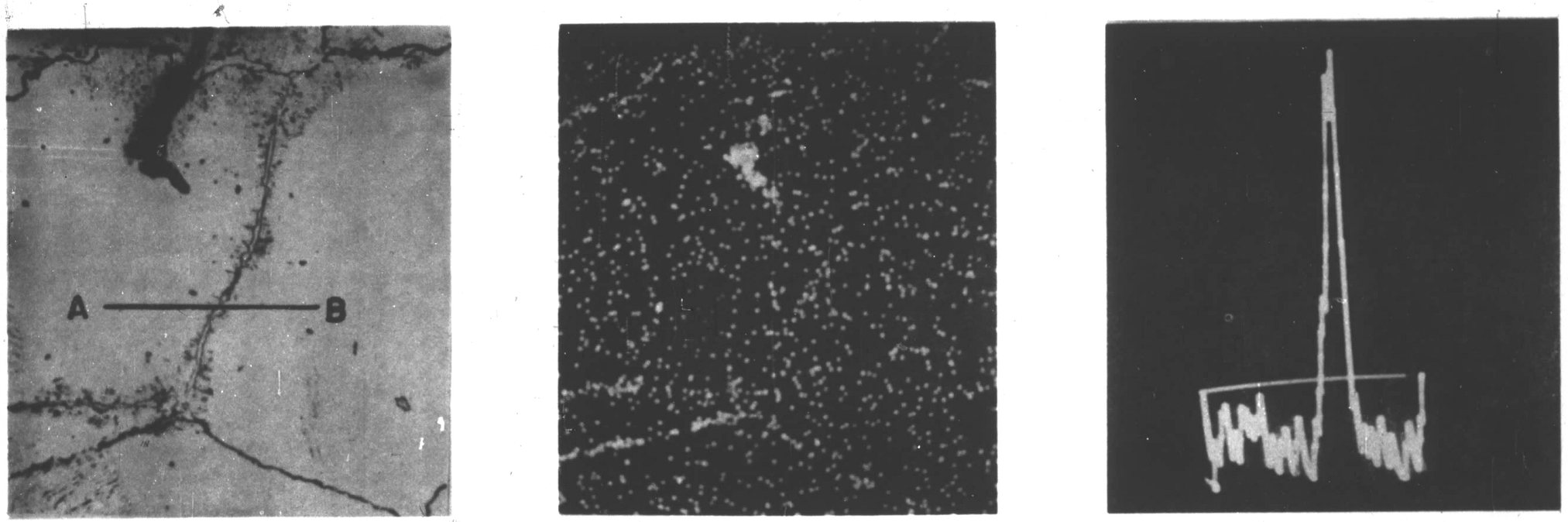

(a) (b) (c)

Figure 18 Micrographs of Ni-Al alloy tested in air (1.0×10^7 cycles). (a) grain boundary behavior as seen in the light microscope, 250X, (b) aluminum x-ray image showing aluminum concentrations at grain boundaries, 250X, (c) aluminum x-ray line scan of line AB of (a). Note: aluminum concentration at peak is 14%, approximately five times that of the bulk material.

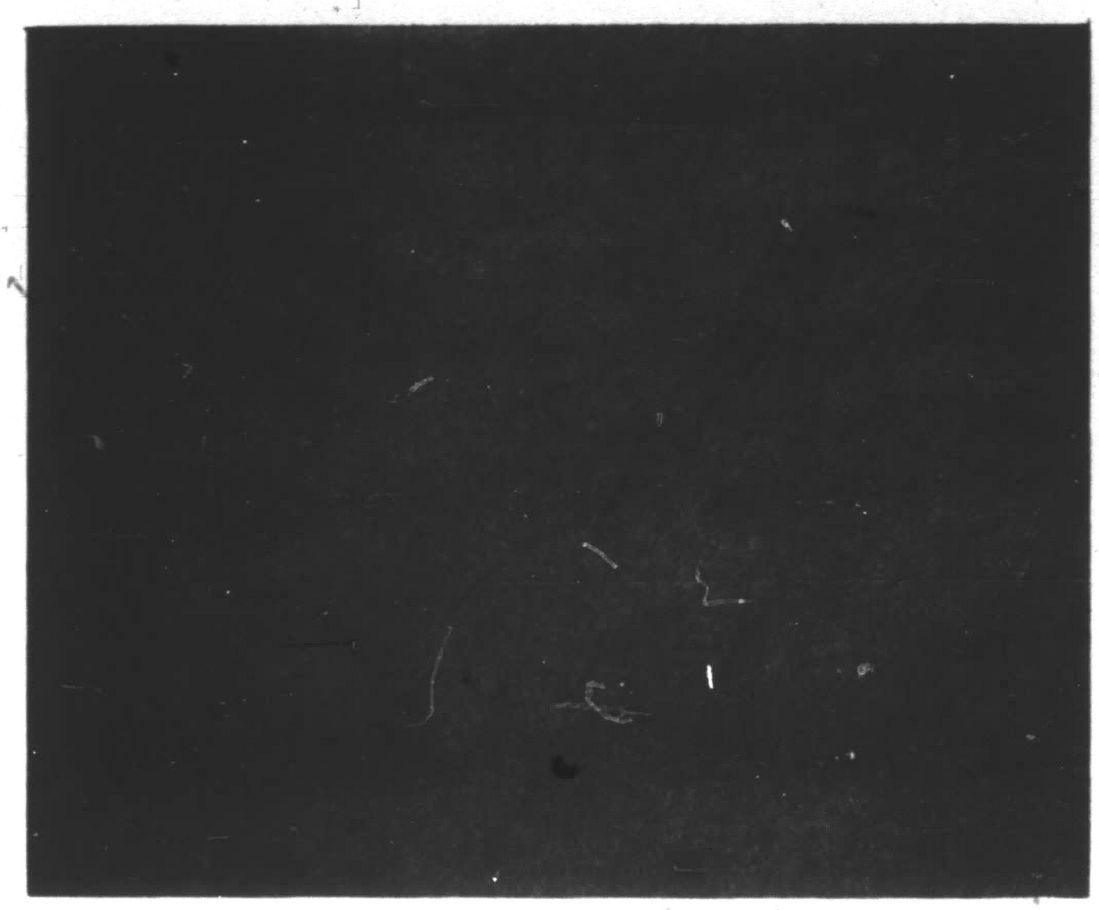

(a)

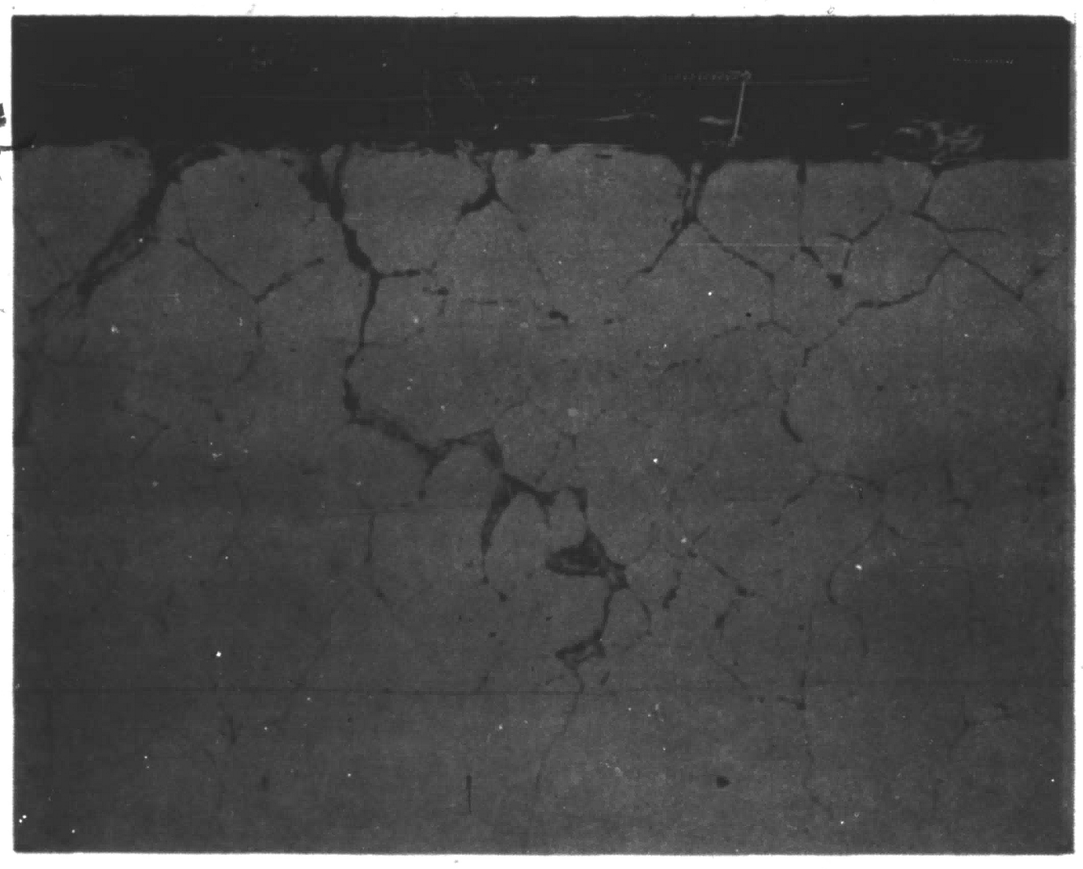

(b)

Figure 19 Oxidation as a result of stressing in air atmosphere. (a) Ni-Al alloy (1.0×10^7 cycles), 50X, (b) Ni-Si alloy (1.0×10^7 cycles), 50X.

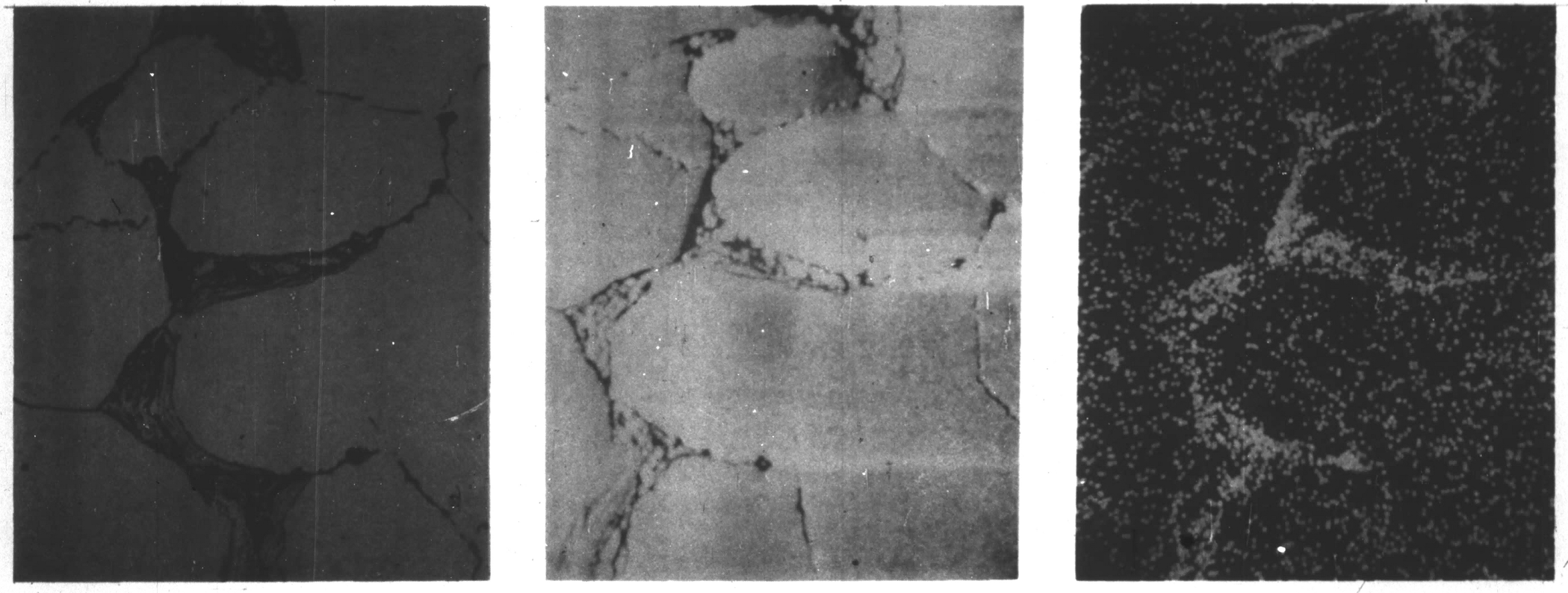

(a) (b) (c)

Figure 20 Micrographs of Ni-Si alloy tested in air (1.0×10^7 cycles). (a) internally oxidized region, 250X, (b) electron image showing structure, 250X, (c) silicon x-ray image showing silicon concentration at grain boundaries, 250X.

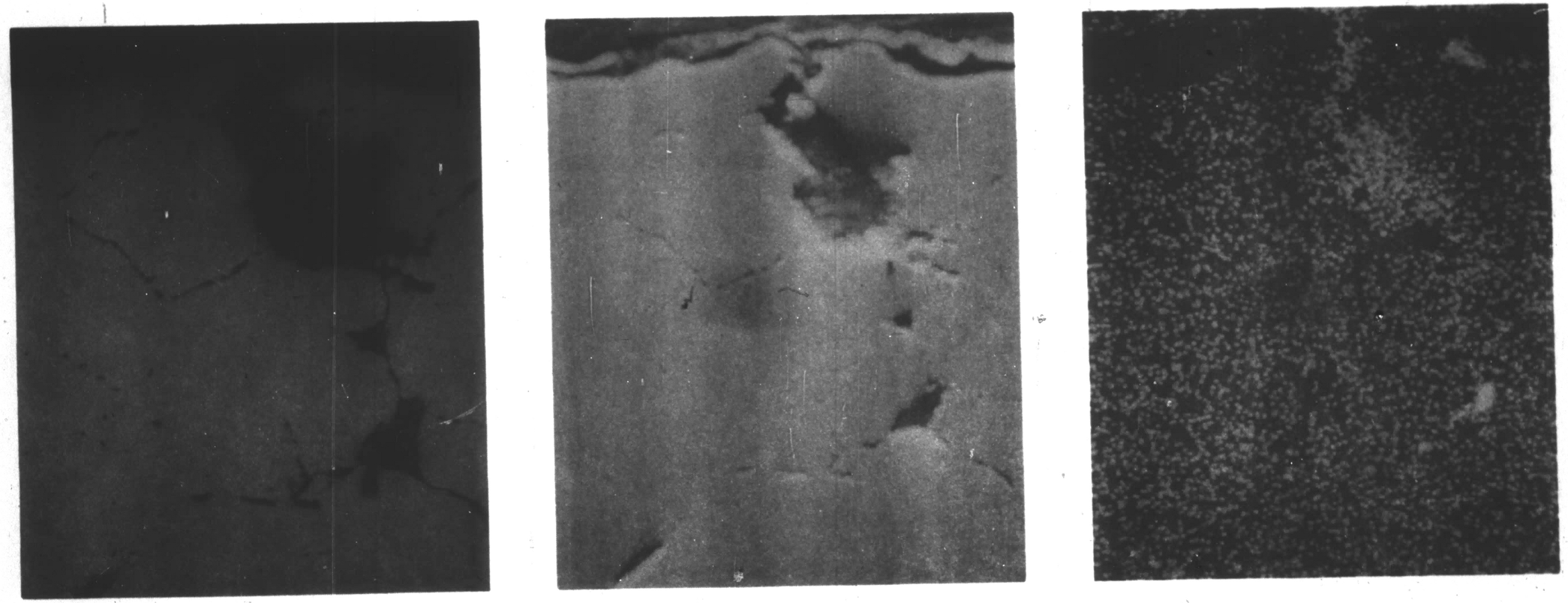

(a) (b) (c)

Figure 21 Micrographs of Ni-Si alloy tested in argon (7.46×10^6 cycles). (a) view of surface and adjacent region, 250X, (b) electron image, 250X, (c) silicon x-ray image, 250X. Note lack of silicon concentration at grain boundaries.

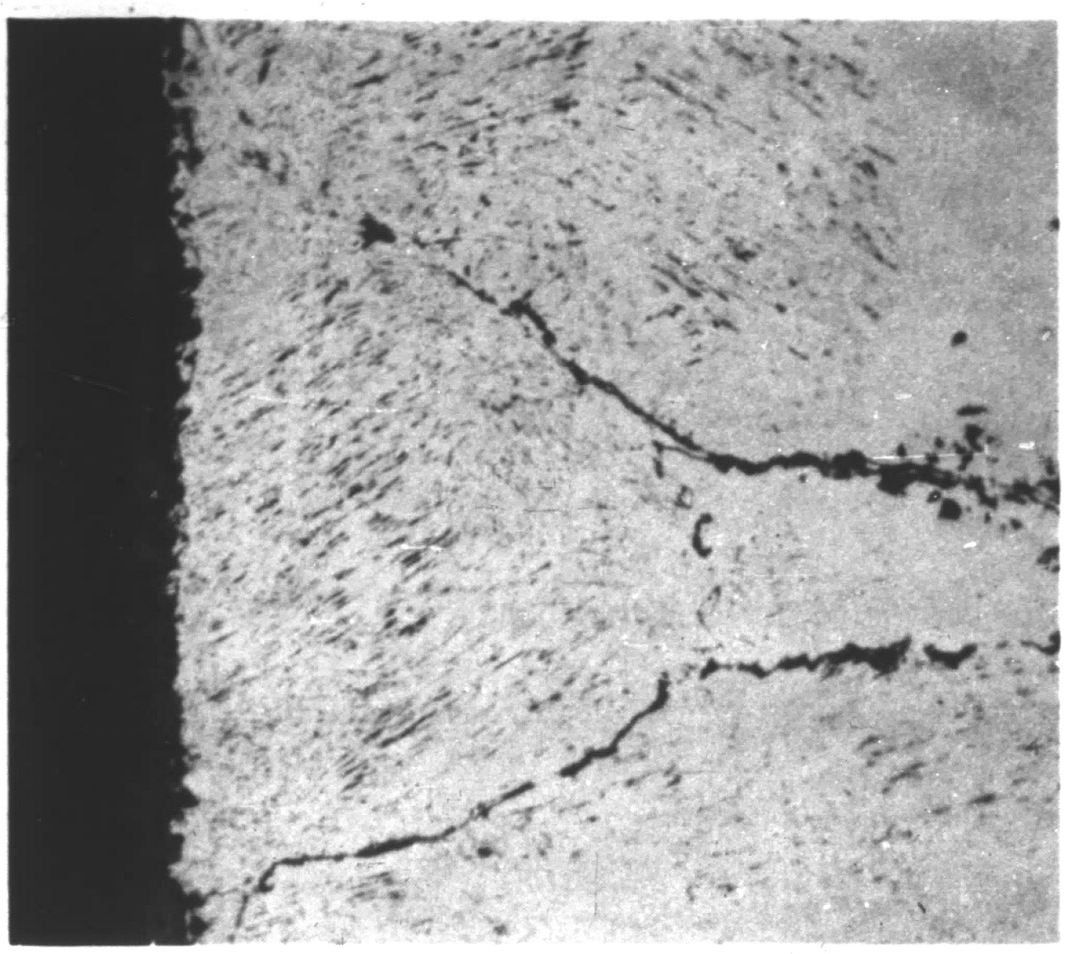

(a)

(b)

Figure 22 Micrographs of Ni-Al alloy tested in air (1.0×10^7 cycles). (a) dispersion of particles below the surface, 500X, (b) view transverse to that of (a), 500X.

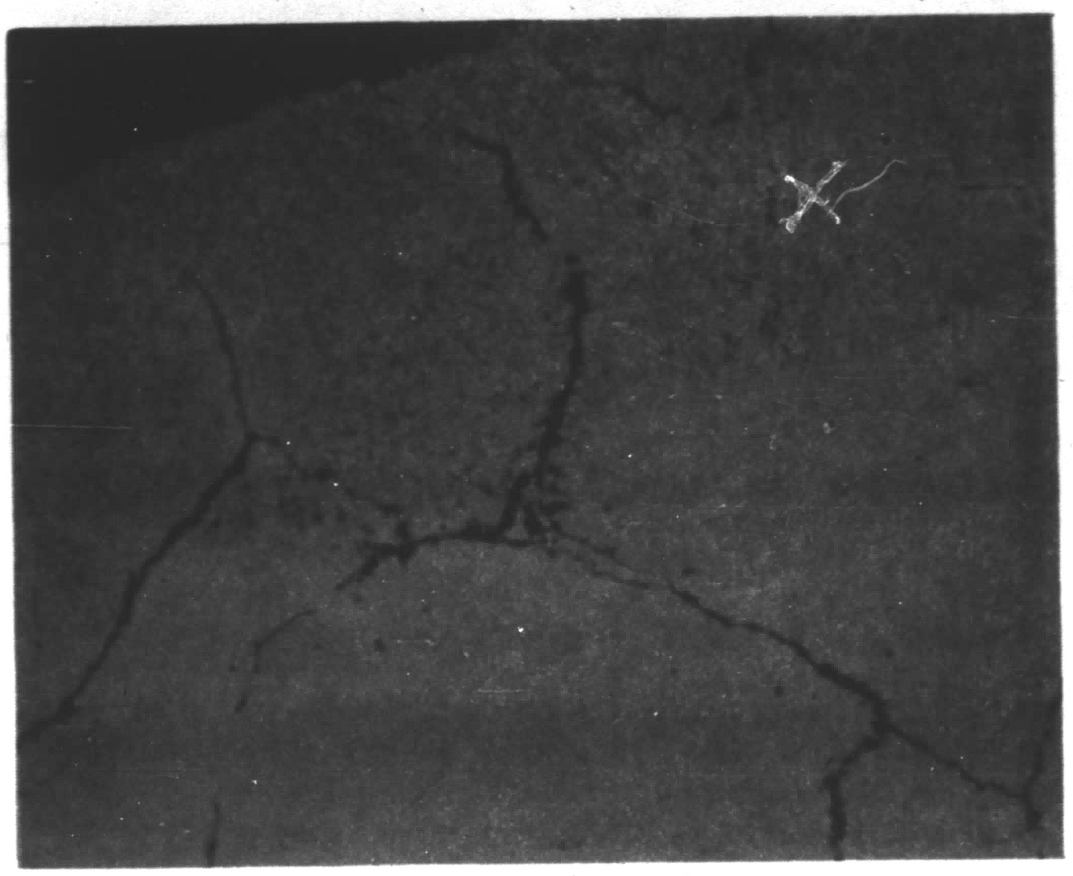

(a)

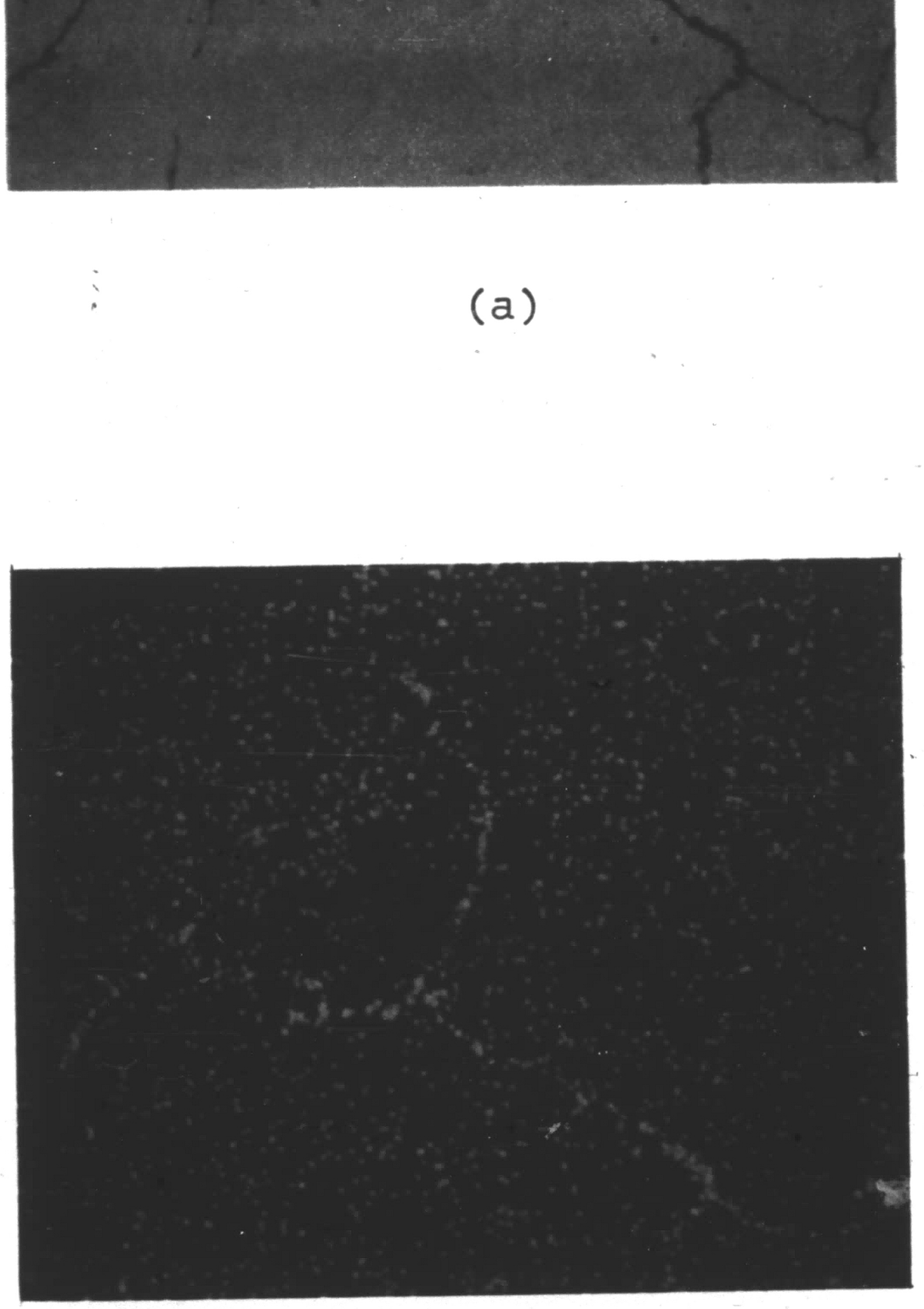

(b)

Figure 23 Micrographs of Ni-Al alloy tested in air (1.0×10^7 cycles). (a) surface and subsurface oxidation, 250X, (b) aluminum x-ray image showing enhanced aluminum content in the region of high particle density, 250X.

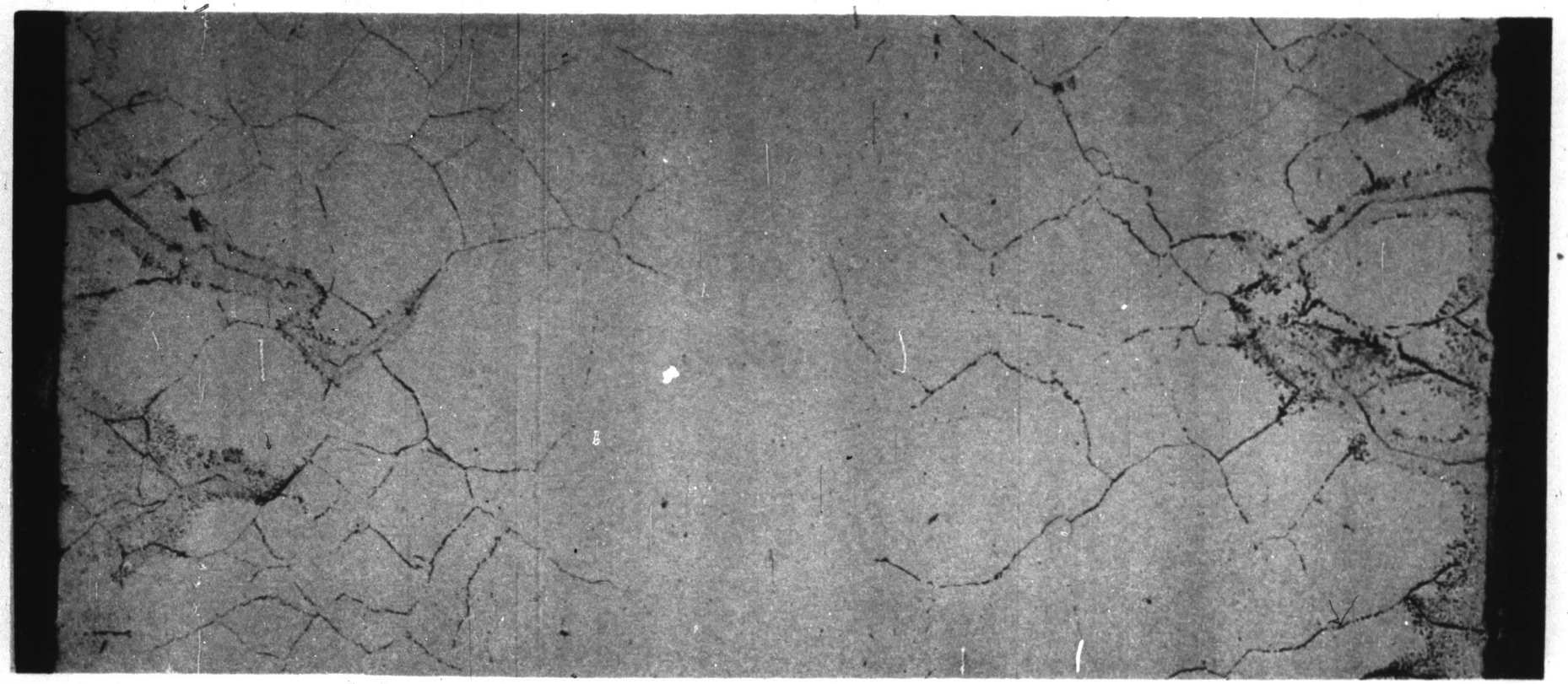

Figure 24 Micrograph of Ni-Be alloy tested in air (1.0×10^7 cycles) showing features of transverse section after testing, 55X.

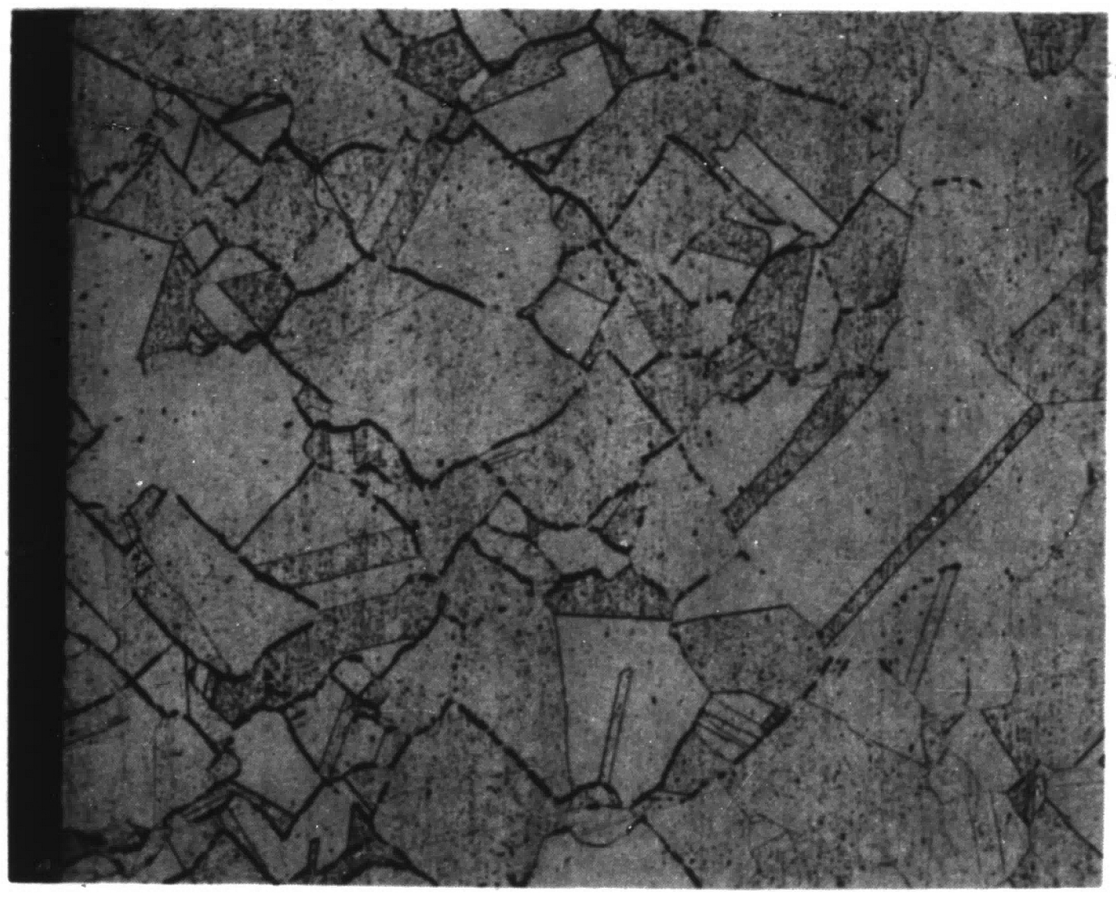

Figure 25 Micrograph of Ni-Al alloy tested in air (7.2×10^4 cycles). Note grain boundary behavior. Etch: HF-HNO_3, 34X.

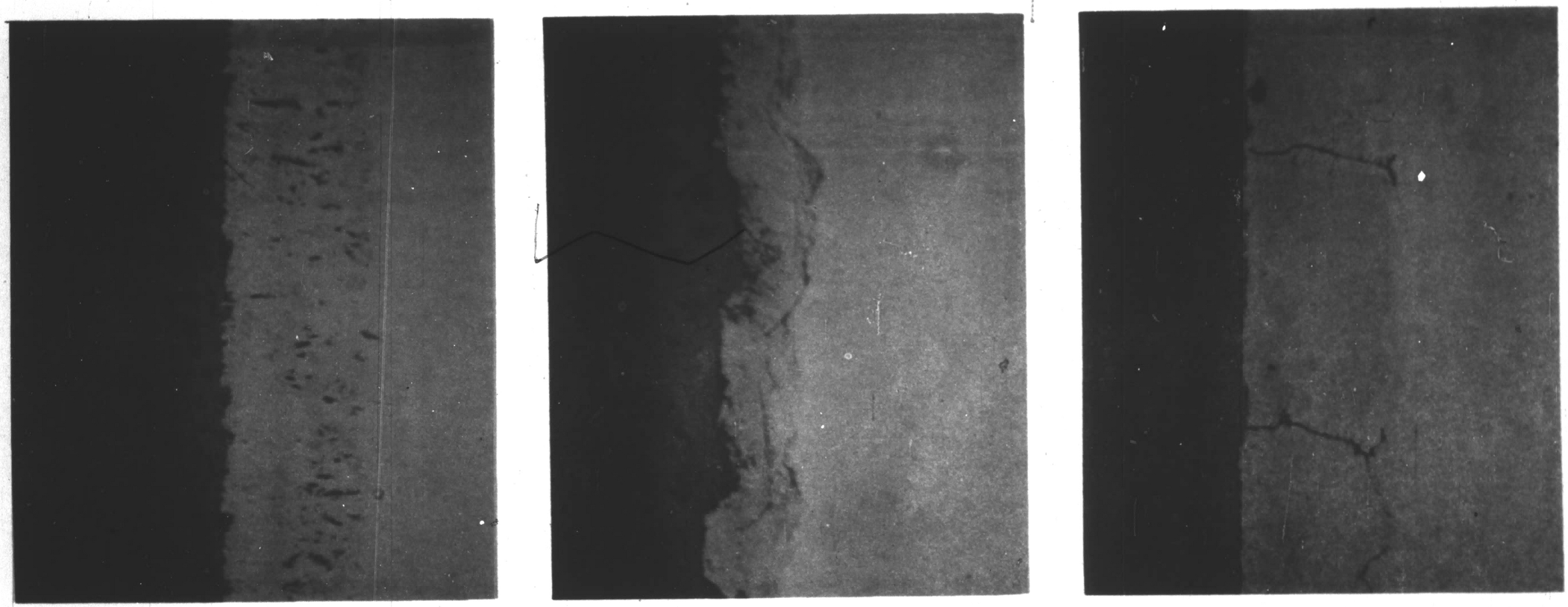

(a) (b) (c)

Figure 26 Oxidation of unstressed material. (a) Ni-Be alloy, 500X, (b) Ni-Si alloy, 500X, (c) Ni-Al alloy, 250X.

Vita

John Herbert Weber, Jr. was born on March 30, 1942 in Norristown, Pennsylvania to J. Herbert and Elizabeth (Krauskopf) Weber. He was educated in the West Norriton Township and Norristown school systems, graduating from A. D. Eisenhower High School, Norristown, in 1959.

In June 1963, Mr. Weber graduated cum laude from Lehigh University with the degree of Bachelor of Science in Metallurgical Engineering. While at Lehigh, he was elected to Tau Beta Pi honorary fraternity, held the Kenneth L. Isaacs Scholarship, received the Allen S. Quier Prize in Metallurgy and was mentioned on the Dean's List. The title of his undergraduate thesis was "Observations on the Fracture Mode and Fatigue Life of Type 304 Stainless Steel at Elevated Temperatures".

Since the completion of his undergraduate studies, Mr. Weber has been engaged in further study at Lehigh University, first as a Materials Research Fellow , and presently as the International Nickel Company Fellow.

In February 1966, Mr. Weber was appointed an Instructor in the Department of Metallurgy and Materials Science at Lehigh University.